Microbial behavior and hydrogen consumption of *Oleidesulfovibrio alaskensis* - Implications for subsurface hydrogen storage

Marte Bertheussen Nåmdal

A thesis written as a part of the *Integrated Master's Program of Energy* at Geophysical Institute

Supervised by Martin Fernø
Co-supervised by Nicole Dopffel and Na Liu
Department of Physics and Technology
University of Bergen
June 1, 2023

Abstract

To reduce global warming an energy transition going from fossil fuel to renewable energy is required and energy storage opportunities to store surplus electricity are needed. Hydrogen gas (H_2) is an energy carrier and can be stored in surface tanks or in geological subsurface formations. Underground hydrogen storage (UHS) offers a large storage capacity suitable for long-term storage. However, high abundance of subsurface microbes using H_2 in their metabolism has undesirable side effects for UHS. Microbes may cause H_2 loss, H_2S formation, and clogging and microbial behavior and H_2 loss mechanisms need to be studied before implementing UHS technology.

This study focuses on how the sulfate-reducing bacteria (SRB) *Oleidesulfovibrio alaskensis* consumes H_2. Laboratory experiments have been performed to increase understanding of how this strain will act in the context of UHS. Suitable storage gas mixtures, the impact of pressure, increasing surface area, and pH were studied to improve the knowledge of SRBs impact on H_2 consumption in the subsurface. Also, a micromodel experiment was performed to investigate the H_2 consumption in porous media.

Generally, the results showed that *Oleidesulfovibrio alaskensis* completely consumed H_2 where the consumption rate was dependent on the growth conditions. More optimal growth conditions increased the consumption rate. A rapid pH increase, above the maximum growth ph of 9, was observed for this strain giving the microbes less optimal growth conditions. Nevertheless, other factors than pH seemed to be more crucial for the H_2 consumption rate for this strain. Investigation of pressure impact showed no significant differences in the H_2 consumption rate, assumingly due to the low pressures used for these experiments. Similar H_2 consumption rates per cm^2 were observed when testing larger gas-liquid contact areas, indicating that larger surface areas are not consuming more H_2 per cm^2. Movements in the aqueous phase seemed to increase the solubility of H_2 causing higher H_2 consumption rates compared to static conditions. In the micromodel experiment, the H_2 consumption stopped before all the H_2 were consumed. The stop in H_2 consumption may be due to the low amount of microbial cells or factors limiting microbial movement like physical hindrances of the pore structure or produced bioproducts inhibiting microbial growth. pH may also affect the consumption in the micromodel but need further investigations.

Obtained results indicate microbial activity in the subsurface as a challenge for UHS. However, research on other SRBs is needed to improve the understanding of how microbes are consuming H_2. Also, core-scale and field-scale experiments are needed to investigate how the microbes are acting under reservoir conditions and in the presence of other chemicals available in the subsurface environment.

Acknowledgements

I want to thank my supervisors Professor Martin Fernø, Doctor Nicole Dopffel, and Doctor Na Liu for their guidance during the work of this thesis. I also would like to express my gratefulness to the reservoir research group at the University of Bergen, for contributions of knowledge, discussion, and insight to the topic of my thesis.

A special thanks to Nicole for her assistance in my laboratory work at NORCE and for discussions of the experimental results. I also want to thank Na for good help in the laboratory work performed at UiB for this thesis.

In the end, I want to thank all my co-student at the University of Bergen for all their support and contribution of knowledge, inspiration, and motivation during all five years.

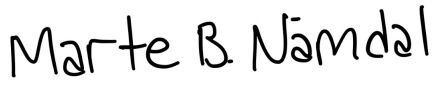

Marte Bertheussen Nåmdal
Bergen, Juni 2023

Nomenclature

P	Pressure	[bar]
V	Volume	$[m^3]$
T	Temperature	[°C]
n	Number of moles	[mol]
R	Gas constant	$[m^3 PaK^{-1} mol^{-1}]$
c	Concentration	[mM]

Abbreviation

AEL	Alkaline electrolysis
CCS	Carbon Capture and Storage
CO_2	Carbon dioxide
FoV	Field of View
GC	Gas chromatography
GHG	Greenhouse gas
H_2	Hydrogen
HHV	Higher heating value
IPCC	Intergovernmental Panel on Climate Chang
LHV	Lower heating value
LOHC	Liquid organic hydrogen carrier
mbarg	Millibar gauge
mmoles	Milimoles
MOPS	3-(N-morpholino)propanesulfonic acid
N_2	Nitrogen
NH_3	Ammonia
PEMEL	Polymer electrolyte membrane electrolysis
SMR	Steam methane reforming
SOEL	Solid oxide electrolysis
TRL	Technical readiness level
UHS	Underground hydrogen storage

Contents

1 Introduction **1**
1.1 Motivation 1
1.2 Objective 3

2 Theory **4**
2.1 Hydrogens's value chain 4
2.1.1 Production 5
2.1.2 Utilisation 6
2.1.3 Storage 6
2.2 Underground hydrogen storage 7
2.3 Microbiology 9
2.3.1 Sulfate reducing bacteria 10
2.3.2 Object of study and microbial growth at laboratory 11

3 Methods **13**
3.1 Methodology 13
3.1.1 Sterile and oxygen-free conditions 13
3.1.2 Make medium 14
3.1.3 Add liquid solutions and gas to closed bottles 16
3.1.4 Pressure measurements 18
3.1.5 Gas composition measurements 18
3.1.6 pH measurements 19
3.1.7 Take liquid sample 20
3.1.8 Acetate measurements 21
3.1.9 DNA extraction 21
3.2 Experimental procedures 22
3.2.1 Growth rate assessment 22
3.2.2 Hydrogen concentration experiment 24
3.2.3 Pressure experiment 25
3.2.4 Surface area experiment 26

3.2.5 pH experiment 28
3.3 Calculations 30
3.3.1 Sensitivity 31

4 Results and discussion **33**
4.1 Growth rate assessment 33
4.2 Hydrogen concentration experiment 34
4.3 Pressure experiment 39
4.4 Surface area experiment 44
4.5 pH experiment 47
4.6 Microbial impact on hydrogen consumption in the porous media 52

5 Conclusion **57**

6 Future work **59**

Appendices **67**

Appendix A HPLC procedure **68**

Appendix B Pressure and gas composition data **70**

Appendix C Calculations for micromodel experiment **72**

Appendix D Sulfate calculations **73**
D.1 Bottle experiment 73
D.2 Micromodel experiment 73

Chapter 1

Introduction

1.1 Motivation

Global warming is a highly relevant challenge humans are facing, and actions are needed. According to Intergovernmental Panel on Climate Change (IPCC), the global net anthropogenic greenhouse gas (GHG) emission in 2019 was 59 $GtCO_2$-eq, about 12 % higher in 2019 compared to 2010 [1]. GHG emissions from fossil fuels and industry had in 2019 the largest growth in absolute emissions [1]. IPCC estimates the remaining carbon budget from 2020 and onwards to be of a size of a fourth-fifth of the cumulative net CO_2 emissions between 2010 and 2019 with a probability of 50 % to limit global warming to 1.5 °C [1]. In 2019, only 11.4% of global primary energy came from renewable energy sources like hydropower, wind, and solar, 4,3% from nuclear, and 84% came from fossil fuel. The global energy mix shows that oil, coal, and gas are the dominating energy sources and renewable energy takes only a small part of this mix [2]. Actions to reduce GHG emission is needed, where the transition going from fossil fuel to renewable energy are a key factor to decrease CO_2 emissions to achieve the climate goals set for 2050 [3]. This transition requires phasing out oil, gas, and coal and building out renewable sources like wind and solar [4].

Renewable sources are inherently variable and intermittent [5] causing a potential mismatch between energy supply and demand. Hence, relying on 100 % renewable energy is challenging without energy storage opportunities [5, 6]. This variability and intermittency increase the need for large-scale energy storage for different time scales to balance the supply with the demand[6, 7, 8]. H_2 is an energy carrier with the potential to substitute fossil fuels [9, 10, 11, 12]. H_2 can potentially be produced, stored, transported, and utilized with low emissions [13, 14]. H_2 can be stored in surface tanks or in underground formations with varied storage capacities. UHS can offer the opportunity to store multi-megawatt of energy needed for future storage of increasing renewable energy production

[4, 15].

UHS is a concept where H_2 is stored in underground geological formations like depleted hydrocarbon reservoirs, aquifers, and salt caverns [7]. It offers the opportunity to store excess energy from renewable sources for a varied amount of time and can be converted back to electricity or other uses when needed [16, 3]. UHS takes advantage compared to other storage technologies of its large storage capacity where huge volumes of gas can be stored [10] and is therefore also a solution for energy security [7]. Compared to surface storage, UHS takes advantage of safety concerns, space management, and availability of suitable storage sites [15]. Experience from natural gas storage can be useful as the design, construction, and operations concept is comparable for both gases [7]. However, the properties of the gases are different and knowledge gaps regarding H_2 behavior and -loss need to be investigated before implementing UHS technology [17]. Figure 1.1 illustrates the value chain of UHS and includes some of the main open questions related to this storage technology [18].

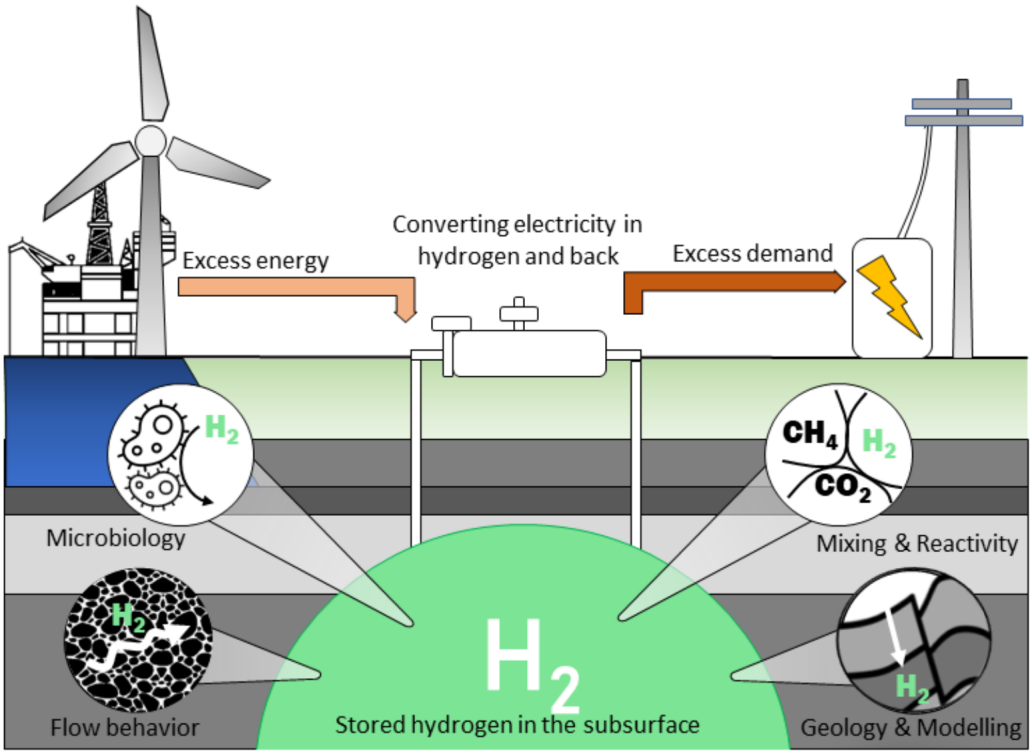

Figure 1.1: Illustration of the UHS value chain [18].

Storage sites relevant for UHS have potentially an abundance of microbes [17]. As microorganisms can use H_2 within their metabolism, subsurface microbes can for example lead to reactions with minerals and H_2S, methane, and acetate production leading to H_2 loss and unfavorable changes in the gas and fluid composition as well as microbial growth causing plugging [17]. Relevant microbial groups for UHS are sulfate-reducers, Methano-

genesis, Acetogenesis, and Iron reducers, as they all consume H_2 and have other side effects related to UHS technology [17, 19]. As H_2 will be in direct contact with the microbes during storage, knowledge of the microbial impact on H_2 needs to be investigated. Recently, more attention and focus on microbial side effects for UHS is observed, but more experience from laboratory experiments and fields test is needed to fully understand the microbial risks related to UHS.

This thesis will focus on sulfate-reducing bacteria and how this microbial group affects H_2 and the surroundings over time. The study will focus on one specific strain, *Oleidesulfovibrio alaskensis*, and how this strain acts with the abundance of H_2. Laboratory experiments will be performed where H_2 gas will be stored in small bottles together with media and microbes. By doing several experiments focusing on the impact of pressure, initial stored H_2 concentration, increasing surface area, and pH, valuable knowledge of the microbial impact on H_2 consumption as well as production of H_2S and pH development will be achieved. The data from performed experiments can be valuable knowledge for further research on this topic and is a step on the road for UHS to be successfully implemented in the future.

1.2 Objective

The overall objective for this thesis is to improve the understanding of how *Oleidesulfovibrio alaskensis* consumes H_2. This knowledge is important for mapping how sulfate-reducing bacterium is affecting H_2 during subsurface storage. More specifically, this study will investigate the following statements:

- As H_2 can be stored in a mix of other gases, it is important to know what gas mix is most suitable for UHS. This knowledge is important to avoid potential H_2 loss and will be investigated in this thesis.
- As geological formations in the subsurface have high pressure, the impact of pressure on microbial activity and hydrogen-consuming processes is of interest. The impact of pressure will be studied.
- In hydrocarbon reservoirs the gas-liquid contact is much larger compared to laboratory bottle experiment and knowledge about H_2 consumption rates at larger surface areas is important.Will the microbes consume more H_2 as the surface area are bigger?
- pH is a factor described to have an impact on the microbial activity as well as H_2S dissolved in liquid [20, 21]. The development of pH and the impact it has on H_2 consumption as well as gas composition regarding H_2S will be investigated.

Chapter 2

Theory

2.1 Hydrogens's value chain

H_2 is the most common element in the universe [22]. Hence, H_2 is very reactive and only exists in compounds such as water and organic materials on Earth. H_2 gas is odorless, colorless, and flammable and can easily leak without noticing leading to some safety concerns [22]. Also, H_2 has a small molecular size with high penetrability and has a diffusion coefficient four times higher than methane [15]. Details about H_2 properties can be found in Table 2.1. H_2 has a significantly higher lower heating value (LHV) than other fuels. To compare, H_2's LHV is 120 MJ/kg at 290 K while gasoline has a value of 44 MJ/kg at the same temperature. However, H_2's volumetric energy density is lower than hydrocarbon fuels. When liquid H_2 has a density of 8 MJ/l gasoline's density is 32 MJ/l. For H_2 gas, the case is the same; gravimetric energy density is higher than hydrocarbon fuels while the volumetric energy density is lower. This means that H_2 gas requires storage tanks of higher volumes compared to hydrocarbon fuels to store the same amount of energy, but more energy can be stored per mass unit [22].

Table 2.1: H_2 properties [15, 22, 23]

Properties	H_2
Molar mass	2.016
Density at NTP $[kg/m^3]$	0.08375
Solubility in pure water at 25 °C and 1 atm	0.0016 g/L
Heating value [MJ/kg]	120-142
Flammability limits [vol% in air]	4-75
Minimum ignition energy [mJ]	0.02
Autoignition temperature [°C]	585
Detonability limits [vol% in air]	11-59
Diffusion coefficient in air at NTBa $[cm^2/s]$	0.61

The state of H_2 is determined by pressure and temperature. The relationship between pressure, temperature, and state of H_2 is shown in Figure 2.1. The graph is showing that liquid H_2 requires low temperatures, more specifically the boiling point of H_2 is -252.9 °C, which means it is energy-demanding to keep the liquid state. Even though, liquid H_2 has an energy density of 70.6 kg/m^3 at -253 °C. At temperatures above -252.9 °C H_2 will mostly appear as a gas, but high pressure will give solid H_2. For H_2 gas higher pressure will increase the energy density. For H_2 storage, liquid or compressed H_2 is more optimal as it achieves higher energy density [15].

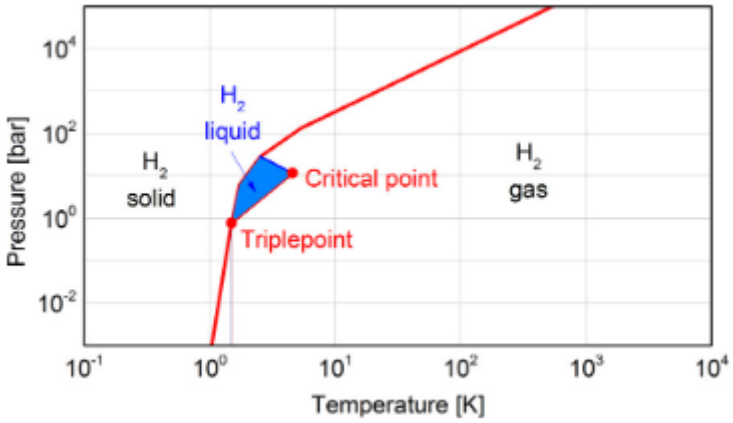

Figure 2.1: H_2 phase diagram [15]

H_2 is an energy carrier, not an energy source, and can potentially be produced, stored, and used with low GHG emissions which makes it highly relevant for the energy transition and low carbon future. The next section is going to give an overview of H_2's value chain.

2.1.1 Production

There are different technologies to produce H_2, with varying CO_2 emissions related to the production. H_2 cleanness level describes the amount of CO_2 emissions related to the production of H_2 and depends on H_2's origin and the technology used for production. H_2 is divided into color codes depending on their cleanness level [22]. Green, blue, and grey H_2 is the type of H_2 of the most attention. Grey H_2 is produced from fossil fuels using technologies like steam methane reforming (SMR), partial oxidation, and autothermal reforming where SMR is the most common technology [24]. Equation 2.1 gives the overall reaction for grey H_2 production, showing that CO_2 is a by-product [25]. In 2020, 99% of the H_2 was produced as grey H_2 [25], and have a levelised cost of H_2 production ranging from 0.5 to 1.7 USD/kg depending on regional gas prices [26]. Blue H_2 is produced the same way as grey H_2, but includes carbon capture and storage (CCS) or carbon capture and utilization (CCUS) technology causing less CO_2-emission [25]. Including CCUS technology in the production of H_2 increases the costs to about 1 to 2 USD/kg

[26]. Green H_2 is produced by water electrolysis using 100% renewable sources [22, 27]. Electrolysis of water is an electrochemical process used to split water molecules into H_2-molecule and oxygen by use of electricity [25]. There are different types of electrolysis, where alkaline electrolysis (AEL), polymer electrolyte membrane electrolysis (PEMEL), and Solid oxide electrolysis (SOEL) is the most used and most common [25]. The benefit of green H_2 is that water is a cheap and an universal raw material and it is an emission-free technology [11]. However, only a small part of H_2 produced today is green due to the high total production cost [11], with a levelised cost of production at 3 to 8 USD/kg [26]. Today, both green and blue H_2 take a small share of H_2 production as the levelised cost for production is high, but it is assumed lower cost for green H_2 than blue H_2 soon and also that green H_2 will be the cheapest alternative in the long term [28]. The overall reaction of green H_2 production is given by Equation 2.2.

$$CH_4 + 2H_2O \rightarrow CO_2 + 4H_2 \tag{2.1}$$

$$2H_2O = 2H_2 + O_2. \tag{2.2}$$

2.1.2 Utilisation

H_2 can either be used in a combustion engine or in a fuel cell. H_2 can contribute to reducing GHG emissions as it can replace the use of fossil fuel in many sectors and has zero CO_2 emissions and minimal air pollution as mostly water comes out during burning of H_2. H_2 can be used in the transport sector and is highly relevant for hard-to-abate transports like trucks, boats, and ships [11]. Also, different industries can use H_2 to reduce GHG emissions. It can be used for ammonia production in the chemical industry as well as the refining process in the refining industry. H_2 can also be used for steel production and to heat up or cool down buildings [11, 22].

2.1.3 Storage

H_2 can possibly be stored both over and under the ground. Which storage site to choose is based on storage time, volume, and end-use. Pipelines and tanks are examples of aboveground H_2 storage sites. H_2 can be stored in different states, either as compressed or liquid H_2. Also, H_2 can be converted to other chemical components and stored as ammonia (NH_3) or liquid organic H_2 carriers (LOHC). Aboveground H_2 storage has a limited storage capacity of 5 to 10 GWh, which fits for storing periods of days or hours [7, 11]. UHS sites can be for example salt caverns, depleted hydrocarbon reservoirs, and deep saline aquifers which have large storage capacities. As H_2 has a high volumetric energy

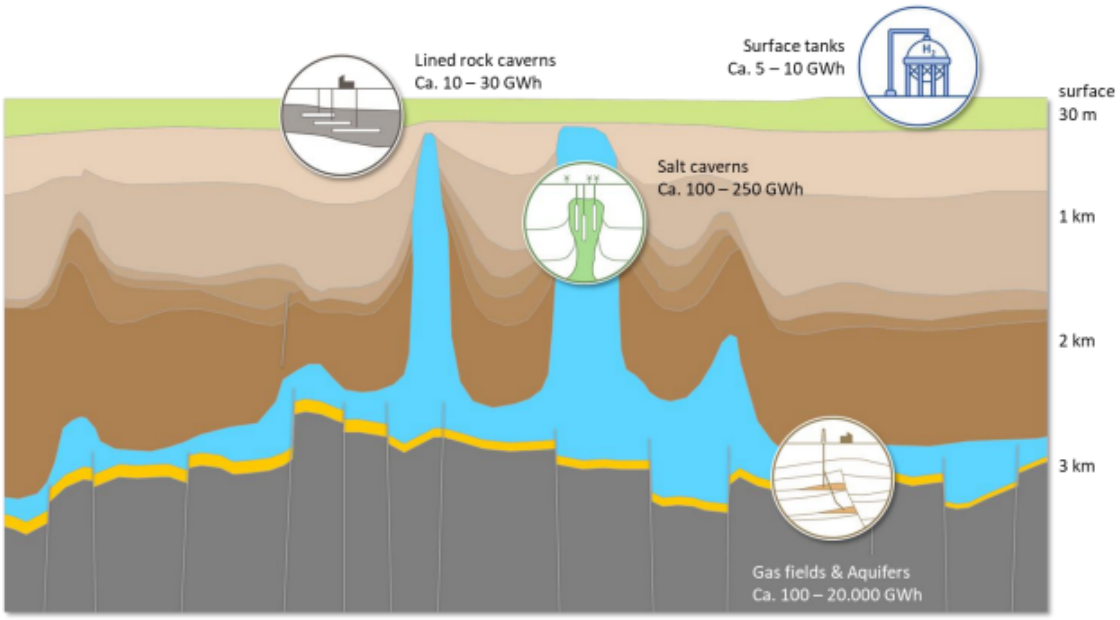

Figure 2.2: A schematic overview of H_2 storage technologies, including assumed ranges for storage capacity [7].

density, large storage volumes are needed to store large amounts of energy. UHS offers this opportunity as well as a long-term storage perspective of seasons or years. However, UHS is not well studied and more knowledge of H_2 behavior and loss mechanisms is needed before implementation. An overview of storage technologies suitable for H_2 storage is given in Figure 2.2 including estimates of storage capacity.

2.2 Underground hydrogen storage

Depleted hydrocarbon reservoirs, deep aquifers, and salt caverns are the three main geological formations suitable for UHS [29]. Each storage site has its own characteristics, but all sites share several fundamental considerations, like for example, sufficient trapping capacity is required for a storage site to be selected. Common for all sites, gas is injected into underground formations and stored as a pressurized gas. The pressure depends on the depth of the storage formation but also on the amount of injected gas, where more gas means higher pressure [30]. Stored gas is distinguished between cushion gas and working gas. Cushion gas is referred to as a permanently stored gas important to keep the minimum pressure while working gas is the gas possible to withdraw and defines the energy capacity of the storage site [30, 31].

Salt caverns are suitable for H_2 storage under high pressure and mostly form through solution mining where water is injected into salt rock forming cylindrical, artificial caverns [29]. The size of a cavern varies, with a diameter from 50 to 100 m and a height between 300 to 500 m, and has a volume ranging from 50000 m^3 to above 1000000 m^3 [9, 29]. A

salt cavern can be built at up to 2000 m depth, where the operating pressure normally ranges from 30 to 80 % of the lithostatic pressure [32]. The operating pressure of a 1000 m deep cavern can exceed 200 bar, while shallow caverns cause lower operating pressure [9]. To avoid salt damage and cavern closure, a minimum pressure is required. At minimum pressure, only cushion gas is present, which for salt caverns represents one-third of the gas volume[9, 30]. For salt caverns, it is possible for up to 10 injection and withdrawal cycles each year, and can therefore be used for more frequent storage [15]. High salt conditions seem to prevent microbial H_2 consumption [33].

Porous media storage, such as depleted hydrocarbon reservoirs and aquifers, uses natural voids where the gas is trapped in an anticline by an impenetrable caprock [9]. Ideally, high porosity and permeability are preferable to ensure high storage capacity and easy injection and withdrawal of fluids through the media [30]. Effective porosity is defined as the ratio between the volume of the connected pores and the total reservoir pore volume and describes the storage capacity of the porous media and permeability describes the [34]. Originally, aquifers are filled with water, and injected H_2 will increase the porous media pressure as no liquid is withdrawn during the injection operation. The injected gas will either displace the liquid downward or to the side due to the lower density of the gas [29]. A disadvantage of storing H_2 in aquifers is the constant change in the liquid-gas interface during the injection of gas, meaning that both liquid and gas can be withdrawn simultaneously [33]. Depleted gas reservoirs can benefit from using the remaining gas as the cushion gas, but it may decrease the H_2 purity due to gas mixing. Depleted oil reservoirs can also decrease the purity of H_2 due to chemical reactions [33]. Storage volumes of porous media are very high [15] where operation pressure as high as 200 bar are common (depending on theoretical conditions and track records) [9]. Unlike salt caverns, porous media storage only offers the opportunity to withdraw the gas for a maximum of two cycles each year [15], and is more suited for seasonal storage.

Properties of H_2 face some challenges for underground storage and can cause H_2 loss and changes in the stored gas mix. As H_2 is a very small molecule with a high ability to diffuse in solid [15], geological tightness is an important factor to consider [35]. The presence of water in the pore space of porous media improves the tightness of these storage sites and as the solubility of H_2 is low in the water, leakage of H_2 is of low risk. The dry walls of salt caverns can potentially cause H_2 diffusion [15]. Contact between H_2 and ambient rocks and minerals can cause chemical reactions and is another potential loss factor as well as decreasing the purity of H_2. Microbes also have the potential for H_2 loss. Some subsurface microbes are known for feeding on H_2, but knowledge of what microbes are triggered by H_2 storage, growth behavior, and possible cons is needed before implementation of UHS [17].

2.3 Microbiology

A microorganism includes all organisms that are smaller than 100 µm and can only be seen in microscopes. Microbes can be either unicellular (single-cell) or multicellular. Microorganisms include bacteria, fungi, archaea, and many other types of eukaryotes [36]. Microbes can be found in all parts of the biosphere where water exists, including high in the atmosphere, in food, and in deep underground formations. Rocks several kilometers deep contain microbes, with cells per gram of rock ranging from 10^4 and 10^8 [37]. The total amount of cells in the continental subsurface is estimated to be 2-6 x 10^{29} [38]. Microbes in the subsurface can originally be indigenous by natural transport or sedimentation processes, or come from human activity like drilling and water injection [39, 35]. Human activity will continue to alter the subsurface conditions, leading to microbial adaption of activity and changes in microbial diversity. The effect of human activity in the subsurface needs to be investigated [17].

Most microbes are beneficial to life, however, pathogenic microbes are harmful and can cause diseases that kill humans, animals, and plants. Microbes are divided into four risk groups, where group 1 and 2 is unlikely or have low risks for human or animal disease while group 3 and 4 are pathogen microbes usually causing serious human or animal disease [40]. Special labs are required for work related to risk group 3 and 4. In Norway, there are only labs qualified for work of risk group 1 and 2, where safety instruction has to be followed to work with risk group 2.

Microbial activity and life depend on access to certain substances and optimal environmental parameters. Water, energy source, and elements such as carbon, nitrogen (N_2), phosphorous, and a variety of trace elements need to be present for microbes to be active and alive [17, 36]. Hence, environmental parameters like temperature, pressure, pH, and salinity affect microbial diversity and abundance growth rate, and chemical composition. Microbes can thrive within temperatures from -15 °C to 121 °C, and pH ranging from zero to 11 [35]. Still, each strain has a range for optimal growth conditions [17]. Microbes are either halophilic, preferring high-salty environments, or halotolerant, thriving in low-salty conditions [41]. The pressure threshold is not clear for microbial activity and ability to survive [17, 36]. Microbial H_2 consuming processes appear where H_2 is in contact with the microbes, which, due to the low solubility of H_2, restrict to the gas-liquid interface [33]. Anyhow, dissolved H_2 will increase the H_2 consumption rate.

Concurrent oxidation and reduction of an electron donor and an electron acceptor gives energy to the microbes [17]. Examples of electron donors in the subsurface can be either simple organic compounds (like acids), complex organic acids (like hydrocarbons), or inorganic compounds. In the subsurface, H_2 is seen as an attractive electron donor due to its low reduction potential [17, 42]. The most common electron-accepting processes in the

subsurface are sulfate reduction, methanogenesis, and acetogenesis and may consume H_2 simultaneously surrounded by high concentrations of H_2. For this process, sulfide (HS^-), methane, and acetate will be produced in the presence of sulfate and CO_2/HCO_3^-. Table 2.2 show details of these H_2 consuming reactions including gained energy for microbes in $kJ*mol^{-1}H_2$ [17]. Subsurface environments like hydrocarbon reservoirs, salt caverns, and aquifers are anoxic, where only anoxic microbes are able to grow dominated by bacteria and archaea [36].

Table 2.2: H_2 consuming process consider to be important for UHS [17, 42]

H_2 consuming process	Reaction	Free energy $\Delta G^0(kJ*mol^{-1}H_2)$
Sulfate reduction	$\frac{1}{4}SO_4^{2-} + H_2 + \frac{1}{4}H^+ \rightarrow \frac{1}{4}HS^- + H_2O$	-38.0
Methanogenesis	$\frac{1}{4}HCO_3^- + H_2 + \frac{1}{4}H^+ \rightarrow \frac{1}{4}CH_4 + \frac{3}{4}H_2O$	-33.9
Acetogenesis	$\frac{1}{2}HCO_3^- + H_2 + \frac{1}{4}H^+ \rightarrow \frac{1}{4}CH_3COO^- + 2H_2O$	-26.1

2.3.1 Sulfate reducing bacteria

SRB are widespread in anaerobic environments and have an optimal temperature for activity at 38 °C [29]. As Table 2.2 shows this microbial group utilizes sulfate as the electron acceptor and H_2 as the electron donor, which generates hydrosulfide (HS^-) [43, 44]. HS^- can be found as hydrogen sulfide (H_2S) or S^2- depending on the pH [45], where H_2S is a toxic gas with a distinguished smell even at low concentrations [9]. The balance between H_2S as a gas and HS^- and H_2S ions is pH dependent. The Bjerrum plot for H_2S (Figure 2.3) is giving the percentage of each component at certain pH [21]. As the graphs show, increasing pH gives a lower H_2S fraction present. Therefore, the development of H_2S content in a closed container can indicate the development of pH.

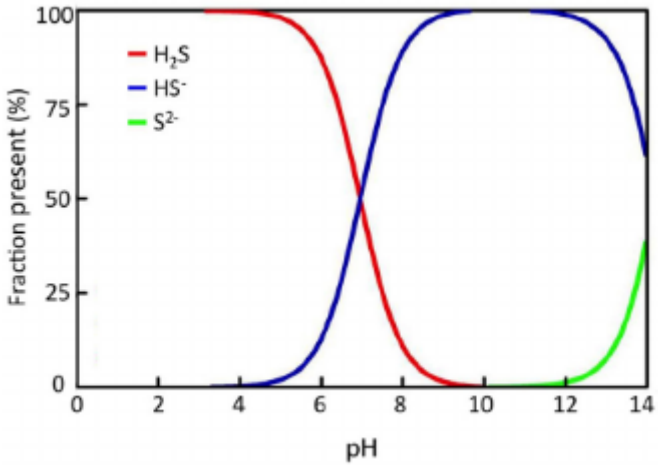

Figure 2.3: Bjerrumplot for H_2S showing the relative fraction in percentage of H_2S, HS^- and sulfide di-anion (S^2-) [46].

pH is a measurement of the acidity or basicity of a solution that measures the concentration of hydrogen ions (H^+) in a solution; $pH = -log[H^+]$. The pH scale ranges from 0 to 14 where pH 7.0 indicates a neutral solution, pH<7 is acid, and pH>7 is basic. High H^+ concentrations give a low pH while low concentrations give a high pH [47]. As the reaction of SRB shows H^+ is getting consumed. The SRB reaction will then lower the H^+ concentration in the solution which will crease the pH. Therefore, the change of pH can indicate the activity of the microbes. As mentioned before, optimal growth conditions for microbes depend on pH and each strain often has a defined minimum and maximum range for growth [20]. Microbial activity can potentially increase the pH above the maximum growth pH. To stabilize the pH a buffer solution can be used. A buffer solution is a solution consisting of a weak acid and its conjugate base and stabilizes the pH of a solution by absorbing the excess ions [47].

2.3.2 Object of study and microbial growth at laboratory

This study will focus on a species within the SRB family named *Oleidesulfovibrio alaskensis*. This bacterium was recovered from a soured oil well in Alaska in 1991 and isolated from material collected by E. van der Vende [48]. It is an anaerobic microbe with bacterial growth temperatures ranging from 10-45 °C, where the optimal temperature is at 37 °C. For *Oleidesulfovibrio alaskensis* a pH ranging from 6.5 to 8.5 will allow bacterial growth, but optimal growth conditions are at a pH equal to 7.0. The optimal salinity conditions for growth is 2.5% but a salinity between 0-10% (w/v) NaCl allows growth. As salt caverns have high salt concentrations, this strain thrives better in porous media sites where the concentration of salt is low. Microbial growth of this strain does not require vitamins, but it is using lactate as an energy and carbon source. Acetate is also a carbon and energy source for this strain. Under optimal conditions, *Oleidesulfovibrio alaskensis* have a maximum growth rate at 0.133 h^{-1} [48]. This strain uses Medium 195c (including some modifications) from DSMZ for growth which has low concentration of salt and are optimized for growth of this strain. *Oleidesulfovibrio alaskensis* was bought from DSMZ, where information on cultivation conditions can be found.

In the laboratory, a method called batch cultures can be used to grow pure cultures. This is a method where microbes grow in closed environments in a fresh medium, like in a laboratory bottle. After being inoculated into new media, it can take some hours before the microbial growth starts. The delay of growth is called the lag phase where the length depends on the strain but also on differences in growth conditions between previous and new conditions. After the lag phase, the microbes often start to grow exponentially. As microbes have some essentials for growth, the cell abundance will stabilise if such resources are limited. This phase is called the stationary phase, where some cells may die while others can continue to grow [36]. Figure 2.4 is illustrating microbial growth in

the laboratory.

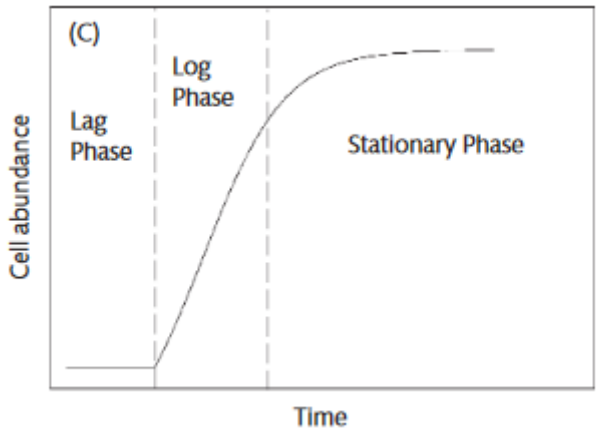

Figure 2.4: Bacterial growth in batch culture, illustrated by the lag phase, log phase, and stationary phase. Modified from [36].

Chapter 3

Methods

This chapter provides an overview of the performed experiments, with details about the experimental setup and performed procedures. It will also give an overview of the equipment and procedures used for the experimental preparations and performance. Experiments were performed in the microbiology laboratory at NORCE main office in Bergen. Performed experiments were following the batch method, where bottles of fresh media and gas mixes of varying compositions of H_2, N_2, and CO_2 were applied. The sampling procedure was performed to investigate the development of H_2 consumption, pH, and H_2S.

3.1 Methodology

This section details the equipment, instrumentation, and routines used in the experimental work. A description of equipment and instruments applications and procedure of use will be given, in addition to other routines used for experimental preparation or performance.

3.1.1 Sterile and oxygen-free conditions

Working with anoxic microbes requires sterile and oxygen-free conditions, which can be obtained using an autoclave. Autoclaves kill microorganisms by using steam under pressure and can be used for both equipment and liquid solutions. The elements are heated to an appropriate sterilization temperature for a given amount of time [49]. The TOMY Multiple Use Autoclaves SX-700E were used and the included manual was followed. To avoid steam inside the articles, like empty bottles, open entries had to be covered with aluminum.

Oxygen-free liquid solutions were also obtained by the following procedure:

1. Weight chemicals and put them into a beaker. Boil distilled water using a microwave and directly flush the water with N_2 afterward to avoid oxygen contamination. Cool down the water to a temperature where the glass beaker can comfortably be touched as to hot water may affect the chemicals.

2. Put approximately half of the water needed into the beaker with chemicals and mix until the chemicals are dissolved. Put the solution into a graduated cylinder and add more water until the desired amount is achieved. When adding more water always add it to the chemical beaker before adding it to the graduate cylinder to make sure you include all of the chemicals. Use a pipette in the end to get the exact amount. If more than three minutes is used from the distilled water going from the original beaker to the final bottle, it has to be flushed with N_2 during the process. This is because liquids can stay oxygen-free for up to three minutes before contamination.

3. Put the solution into the storage bottle, flush the headspace of the bottle with N_2, put on a rubber stopper, and secure the bottle with a vial cap lid using a crimper to make sure it stays oxygen-free. The solution needs to be autoclaved if it is not going to be used within one to two days to make sure it is fully oxygen-free.

3.1.2 Make medium

A modified version of Medium 195c from DSMZ was used for performed experiments. The medium had to be made and prepared in laboratory bottles before the experiments started. To make medium, solution A to F (Table 3.1) needs to be mixed together in a widdel flask (Figure 3.1) under sterile and anoxic conditions.

A stock solution of Solution A was at the beginning of the lab work to save time when making new batches of media. The stock solution contained 10 times each compound, except selenite-tungstate solution and Na-resazurin solution, and was mixed with 1000 mL distilled water. The selenite-tungstate solution was not used in the media, while the Na-resazurin solution was added later. The stock solution was stored at 8 °C until new batches of medium were made. The following steps were performed to make medium:

1. Put 100 mL stock solution and 900 mL distilled water into the widdel flask together with a magnetic stirrer. The widdel flask is illustrated in Figure 3.1, but the experimental set also included a gas port/line connected to port 2. Prepare the widdel flask to be autoclaved by tightening port 3 and 2, closing the valve on the gas line connected to port 2, covering port 5 with aluminum, tight the clamp, and putting on the lids for port 1. The lids at port 1 must be a bit open to let the pressure go out somewhere when the temperature increases in the flask. Autoclave the widdel flask. It is important to take out the flask before the temperature goes

Table 3.1: Solutions A to F including all compounds for medium 195c. The medium made for these experiments included some modifications: Selenite-tungstate solution and Solution D (marked in red) were not added and 0.25 mL Na-resazurin (0.2 % w/v) was used instead of 0.5 mL Na-resazurin (0.1 % w/v).

Solution	Compound	Amount	Unit
Solution A	Na_2SO_4	3.00	g
	KH_2PO_4	0.20	g
	NH_4Cl	0.30	g
	NaCl	21.00	g
	$MgCl_2$ x 6 H_2O	3.00	g
	KCl	0.50	g
	$CaCl_2$ x H_2O	0.15	g
	Selenite-tungstate solution	1.00	mL
	Na-resazurin solution (0.1 % w/v)	0.50	mL
	Distilled water	920.00	mL
Solution B	Trace element solution SL-10	1.00	g
Solution C	Na_2CO_3	1.50	g
	Distilled water	30.00	mL
Solution D	Na-L-lactate	2.50	g
	Distilled water	10.00	mL
Solution E	Wollin's vitamin solution	10.00	mL
Solution F	Na_2S x 9 H_2O	0.40	g
	Distilled water	10.00	mL

under 80 °C and to start flushing the flask with a gas mix of 80% N_2 and 20% CO_2 within three minutes to avoid oxygen contamination. Connect the gas line to port 2 and open the valve to let the gas in. During flushing, it is important to keep port 1 a bit open to let the pressure out. Turn on the magnetic stirrer to obtain a good mix of the solution in the widdel flask.

2. Add the given amount of solution B, C, E, F, and Na-resazurin solution. The Na-resazurin solution used had 0.2 % w/v, therefore, only 0.25 mL was added. Port 1 to the right is used for adding solutions and a burner has to be on when opening any entries to keep sterile and oxygen-free conditions. Wait 30 to 60 minutes for the solutions to mix completely.

3. Measure and adjust pH. 1000 µL samples are taken from the left port 1 by use of a Eppendorf pipette and measured by the electrode pH-meter (see section 3.1.6). The pH is supposed to be in the range of 7.1 - 7.4. Adjust pH by adding acid (HCl) to lower the pH or base ($NaOH$) to higher the pH.

4. Fill bottles. Port 5 is used to fill the bottles. The lids to port 1 need to be closed to get overpressure in the flask to push the liquid up the line inside the flask. Turn on the burner, and slowly open the crimp to fill the bottles. Fill the bottles with

the wanted amount and close the bottles with the stopper and secure the bottle with a vial cap lid using a crimper. Before filling, the bottle tip has to be burned as well as the stoppers to keep sterile and oxygen-free conditions. Flush the bottle headspace with the gas mix of N_2 and CO_2 before closing the bottle.

Bottles of 58 and 117 mL were filled during media making. For the 58 mL bottles, 25 mL media was filled, while 50 mL media was filled in the 117 mL bottles. After preparing the media, the bottles were stored at 7 °C until the experimental start.

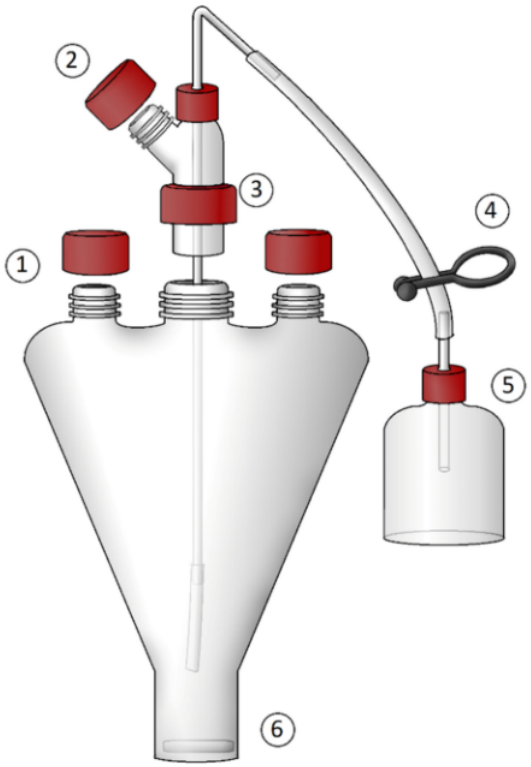

Figure 3.1: A schematic illustration of the widdel flask. Port 1 was used for inputs (right) and outputs (left), and port 2 was where the gas line was connected to flush with O_2-free gas. 4 is illustrating a clamp used for media filling. Port 5 is where the media came out when bottles were filled. 6 is illustrating the magnetic stirrer [50].

3.1.3 Add liquid solutions and gas to closed bottles

When adding liquid solutions to a closed bottle following procedures had to be followed:

1. Use a syringe to take out the desired amount from the liquid solution. Make sure there is no gas in the syringe before adding the solution to the bottle. Inject the solution to the liquid phase to avoid gas dissolution.

Two methods were used to change the gas composition and increase pressure in closed bottles. The syringe method used a syringe for this purpose, while the gas line method

used the gas line directly. The gas line method is favorable when replacing the whole gas composition and was used to add small (>500 mbar) pressure to the bottles, while the syringe method was more suitable when adding an exact amount of gas and increasing the pressure up to 2 bar. The procedure of syringe method was as followed:

1. Turn on the gas line and flush the syringe three times with the same gas mix as adding to the bottle to be sure there are no other gases in the syringe. Flush the syringe by filling it up with the gas mix before pushing out the gas.

2. If the purpose is to exchange the gas composition without adding pressure, first take out the same volume of gas from the bottle as planned to inject, before adding gas. If the purpose is to increase pressure, gas can be added directly. Add gas by filling the syringe to desired amount, and inject the gas into the gas phase of the bottle using a needle. Take the needle out carefully to make sure the stopper is tight and no gas leaks out of the bottle.

The gas line method had the following procedure:

1. Turn on the gas. Put the gas line needle into the bottle directly and immediately put in a disconnected needle (see Figure 3.2) to exchange the gas in the bottle.

2. Flush for x minutes to exchange all the gas. x depends on the volume of the gas phase but ranges from one to five minutes. One minute was used for the 58 mL bottles.

3. Take out the disconnected needle before the gas line needle to avoid air contamination but be fast to avoid increased pressure.

Figure 3.2: Illustration of how the gas line method is flushing the bottle using a needle connected to the gas line and a disconnected needle to exchange the gas composition.

3.1.4 Pressure measurements

A pressure transducer was used to measure bottle pressure. A needle connected to the pressure transducer is pushed into the overhead space which measures and convert pressure into an electrical signal. Figure 3.3a illustrate pressure measurements. Sampling was performed under a fume hood for safety reasons.

3.1.5 Gas composition measurements

The gas composition of a bottle headspace was measured using a Micro Gas Chromatography (microGC), named Agilent 490 Micro GC, including the Soprane software. Standard instructions for use were followed and sampling was performed under a fume hood for safety reasons. A needle connected to the microGC took out a 200 µL sample and the percentage of each gas present in the bottle was given. Figure 3.3b illustrates gas composition measurements and the data was logged on a computer. The Agilent 490 Micro GC can measure the gas composition of bottles having pressure ranging from 25 to 1000 millibarg (mbarg). An overpressure of 25 mbarg is required to avoid the bottle to suck in gas from the microGC, while the maximum sample inlet pressure is specified for this specific instrument.

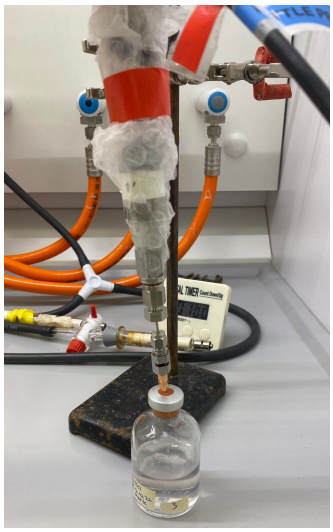

(a) Illustration of pressure measurements using a pressure transducer.

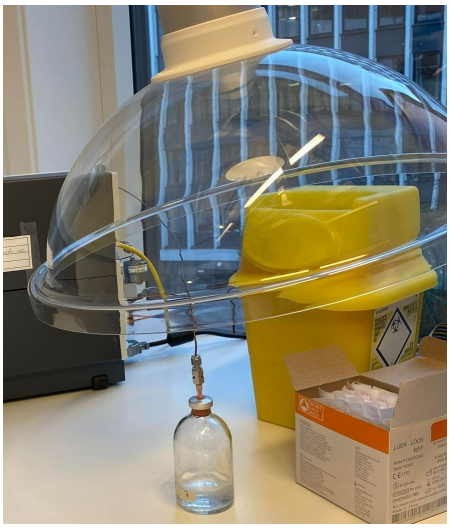

(b) Illustration of gas composition measurements using a microGC.

Figure 3.3: Instruments used for pressure and gas composition measurements.

3.1.6 pH measurements

Two different pH meters were used for pH measurements. The compact pH meter, Horiba LAQUAtwin model 11 with an accuracy of ± 0.1 pH (Figure 3.4b), took advantage of small sample volumes and was used for sampling pH in the experimental bottles. The electrode pH meter (Figure 3.4a), WTW inoLab pH 720 Set, required bigger sample volumes and was used for pH adjustments during media making when the sample size didn't matter. The accuracy for the electrode pH meter was ± 0.01 pH. The sampling routine for the electrode pH meter was as follows:

1. Put a sample of 1000 µL into a centrifuge tube using an Eppendorf pipette. Clean the electrode using distilled water to avoid contamination.

2. Put the electrode down in the sample, stir and wait until the pH is stable before reading the pH.

The Horiba LAQUAtwin pH meter always had to be calibrated before use. A pH 7.00 buffer was used for this calibration and included instructions were followed. To use the compact pH meter for pH measurements, the following steps were followed:

1. Take a 200 μL sample using a syringe and add it to the sensor area. Shake the pH meter carefully and wait until the pH is stable before reading the pH.

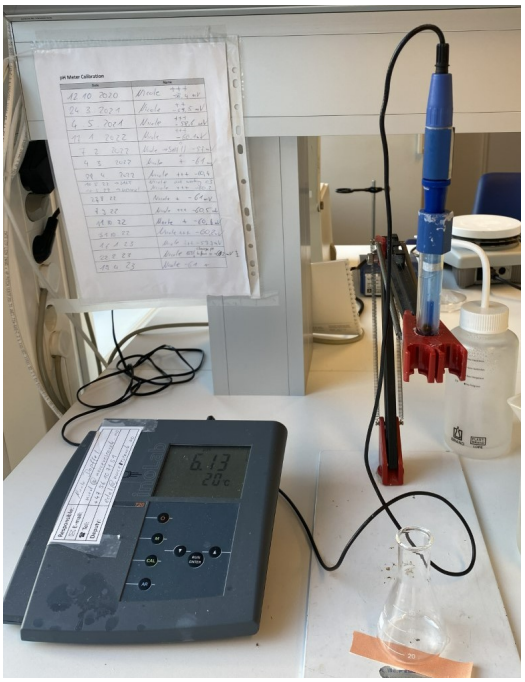

(a) The electrode pH meter used for pH adjustments during media making. The electrode is stored in a ... solution when not used and has to be cleaned with distilled water before pH measurements.

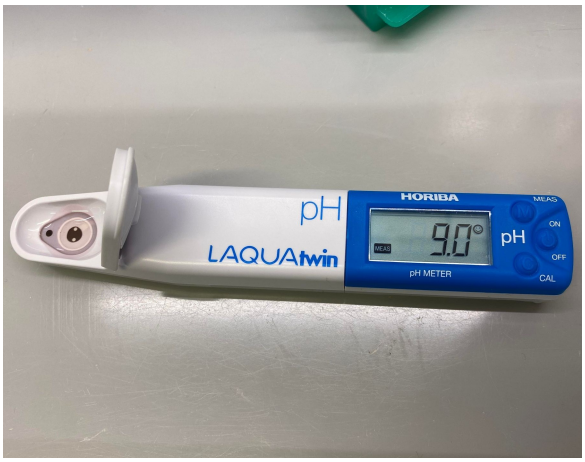

(b) The compact pH meter used for pH measurements from bottle samples. The sensor area had to be cleaned with paper in between different samples.

3.1.7 Take liquid sample

Liquid samples were taken from the experimental bottles (often at day 0 and at the end of an experiment) and were for the purpose of doing DNA extraction and measuring cell numbers but also for Liquid chromatography to measure acetate. The liquid samples were stored at - 20 °C until further measurements. The procedure of taking liquid sample was as followed:

1. Take out a 1 mL sample from the bottle using a syringe, put it into a microcentrifuge tube, and close the lid.

2. Centrifuge the tube for 20 minutes at 13000 rounds per minute (rpm) using the Heraeus Biofuge Pico to gather the DNA in the bottom of the tubes.

3. Separate the liquid (supernatant) from the solid (pellets) using an Eppendorf pipette to slowly take out the supernatant. Fast movements will cause turbulence and may dislodge the pellets and mix with the liquid. Take the supernatant into a new microcentrifuge tube.

4. Store both the supernatant and pellets in the freezer at - 20 °C.

3.1.8 Acetate measurements

High-performance liquid chromatography (HPLC) is a technique used to analyse the liquid composition of a sample [51]. The HPLC measurements were performed to measure the acetate concentration in the bottles to see if acetate was consumed during the experiments. Other components could be calculated but were not of interest in this study. The HPLC procedure and calculations were performed by Dr. Abduljelil Kedir but preparation for the HPLC measurements was performed by myself. The HPLC procedure can be found in Appendix A. The preparation step was as follows:

1. Defrost the supernatant.
2. Dilute 500 µL of the liquid sample by 1000 µL of the mobile phase solution, 14 mM H_2SO_4, in a microcentrifuge tube.
3. Put the solution into a vial using a syringe and a 0.45 µL RC syringe filter and close the lid. The samples are now ready for liquid chromatography.

break up cell

3.1.9 DNA extraction

DNA extraction was performed to measure the concentration of DNA in the bottles. The liquid sample containing the pellets was used for this purpose. The data and final samples from the DNA extraction are going to be used for cell number measurements. Due to time limitations, cell numbers were not measured for this thesis, but will be for a later publication. The DNA extraction was performed but collected data will not be of focus in this thesis. The DNA was extracted by the following procedure:

1. Give the samples a pre-treatment of ultrasonic waves and deep freezing to remove contaminants and impurities and improves the efficiency and purity of the DNA extraction. First, give the samples a bath in ultrasonic waves for five minutes, before putting the samples in a -80 °C for five minutes, and end with redoing the bath in ultrasonic waves for five minutes.
2. Follow the procedure for DNeasy Blood & Tissue by QUIAGEN. Some modification was done: 13000 rpm instead of 14000 rpm due to limitations of the centrifuge used, 50 µL water instead of 100 µL of solution AE.
3. Invitrogen Qubit 4 Fluorometer by Thermo Fisher Scientific is used to measure DNA concentrations and needs to be calibrated before use. Calibrate the instrument by measuring two standards, one high concentration, and one low concentration. The standards are made by mixing 190 µL working solution with 10 µL standard solution. Mix by vortex for three to five seconds and incubate at room temperature

for two minutes before measuring the DNA concentrations for the standard.

4. Prepare the DNA solutions by taking 99 µL working solution and 1 µL of the final samples (from the DNA kit) into a special microcentrifuge tube. Mix the solution by vortex for three to five seconds and incubate at room temperature for two minutes. Measuring the DNA concentrations DNA solutions.

3.2 Experimental procedures

This section provides an overview of performed experiments including the objective, experimental setup, and sampling routine. In general, the experiments was performed to investigate how *Oleidesulfovibrio alaskensis* behaved and consumed H_2 under different conditions. For all experiments, the bottles were stored in an incubator at 37 °C and were temporarily removed for sampling. The sampling procedure varied according to the experimental conditions, but for most experiments, pressure, gas composition, pH, and liquid samples were measured to study the H_2 consumption and follow the growth conditions in the bottles. For most experiments, the bottles were stored upside down (with stoppers on the bottom) to avoid gas leakage through the stoppers.

Before starting any experiments, medium was made by following the procedure described in section 3.1.2. Also, a preculture was made before each experiment were medium 195c. was inoculated with cells of *Oleidesulfovibrio alaskensis*. The preculture was cultivated under ideal growth conditions for three days. A preculture is an pre cultivation of microbes made to grow up a small population of microorganisms under suitable growth conditions, to obtain a sufficient amount of biomass [52]. This is to be sure the microbes are active when starting the experiment. The preculture was made using one of the 117 mL volume bottles filled with 50 mL medium, were 600 µL lactate and 2 mL bacterium culture were added as described in section 3.1.4. The preculture was stored at the 37 °C incubator for three days before the experimental start. Before inoculating the preculture into the bottles, the gas composition was sampled to quantify the amount of H_2S in the preculture.

3.2.1 Growth rate assessment

Prior to experimental research, investigations of the growth pattern related to the specific strain of study are important to determine the sampling frequency during experiments. The objective of this experiment was to assess the growth rate of *Oleidesulfovibrio alaskansis* and to learn the sampling procedure for the upcoming experiments.

Two bottles of 58 mL volume filled with 25 mL medium were used for the growth rate assessment having concentrations of 10 % and 90 % H_2 in the headspace. First acetate

and inoculum were added to the medium bottles following the procedure described in section 3.1.4 before the gas was added. For the 10 % bottle, H_2 was added using the syringe method. To obtain 10 % H_2 in the bottle, 5 mL of the gas had to be exchanged with H_2. Then, the gas layer contained a gas mix of H_2, CO_2, and $N2$. N_2 was used as it do not effect the hydrogen-consuming processes. For the 90 % bottle, the gas line method was followed. The bottle was flushed for 1 min, before 5 mL of the gas was exchanged with CO_2 using the syringe method. CO_2 is added as Medium 195c is described to have CO_2 in the gas mix. More detail of the bottle set-up can be seen in Table 3.2.

Table 3.2: Experimental bottle set up for growth rate assessment.

H_2 % of headspace	CO_2 % of headspace	N_2 % of headspace	Media [mL]	Acetate [µL]	Inoculum [mL]
10	10	80	25	250	2.5
90	10	0	25	250	2.5

The duration of the growth rate assessment was seven days, where pressure and gas composition were sampled daily (except Day 5 and 6; no access to the laboratory). Pressure and gas composition were sampled to calculate the content of H_2 in the headspace in mmoles at a certain time and was sampled daily to be able to follow the H_2 consumption. Details about the calculations can be found in section 3.2.6. During sampling, gas was lost due to small samples taken for each measurement. As the study wants to investigate the H_2 consumption, sampling loss has to be subtracted. To be able to calculate sampling loss pressure was sampled both before and after gas composition measurements. Details about calculating sampling loss can be found in section 3.2.7. The sampling stopped on day 4 or before if all H_2 was consumed. At day 0 pH was measured before sampling of pressure and gas composition started. When the bottles were done or sampling stopped, pH was measured after pressure and gas composition measurements to get an impression of how the pH developed for this strain.

The pressure was held at around 100 mbarg during the experiment. The pressure decreased during the experiment due to microbial H_2 consumption and gas loss during sampling. As the microGC requires over-pressure in the bottle, the pressure sampled before the gas composition always has to be over 25 mbarg. If the pressure were under 25 mbarg the bottles had to be pressurized using nitrogen. Nitrogen is only contributing to increasing the bottle pressure and is not affecting the bacterial H_2 consumption. Nitrogen is added using the syringe method, and the amount added depends on the pressure in the bottle. If there were under pressure in the bottles more nitrogen had to be added compared to if there was 10 mbarg pressure.

3.2.2 Hydrogen concentration experiment

As it is an ongoing debate about the suitable gas mixture to be stored for UHS, an experiment investigating how different H_2 concentrations in the gas mix impact the H_2 consumption rate was performed. Bottles of varying concentrations of H_2 were used and the H_2 consumption was followed daily to notice the impact.

14 bottles of 58 mL volume filled with 25 mL medium were used for this experiment. Concentrations of 0, 10, 40, and 90 % H_2 in the headspace were used and each concentration had duplicates of unsterile and sterile bottles (exept the 0 % H_2 concentration). Acetate and inoculum were added to the bottles as described for the growth rate assessment, as well as the gas mix 10% and 90% H_2. For the 0% H_2 concentration bottles, no gas was exchanged. To obtain 40% H_2 concentration, the syringe method was used to exchange 20 mL of the gas mix with 20 mL H_2. More details about the bottle set-up can be found in Table 3.3.

Table 3.3: Experimental setup for the hydrogen concentration experiment.

H_2 % of headspace	CO_2 % of headspace	N_2 % of headspace	Medium [mL]	Acetate [µL]	Inoculum [mL]
0	10	90	25	250	2.5
0	10	90	25	250	2.5
10	10	80	25	250	2.5
10	10	80	25	250	2.5
40	10	50	25	250	2.5
40	10	50	25	250	2.5
90	10	0	25	250	2.5
90	10	0	25	250	2.5
sterile 10	10	80	25	-	-
sterile 10	10	80	25	-	-
sterile 40	10	50	25	-	-
sterile 40	10	50	25	-	-
sterile 90	10	0	25	-	-
sterile 90	10	0	25	-	-

The concentration experiment lasted for 7 days and the sampling routine and procedure of pH, pressure, and gas composition were similar to the growth rate assessment. Also, liquid samples were taken for this experiment at the same time as pH was measured. For this experiment, the sampling continued until all the H_2 were consumed. The sampling of the sterile bottles stopped when the unsterile bottles of the same initial concentration were finished. Also, the pressure was held at around 100 mbarg pressure and the procedure of pressurizing with nitrogen when the pressure was too low, was the same.

3.2.3 Pressure experiment

As UHS sites operate under high pressure (around 200 bar), knowledge of pressure impact is important. Higher pressure may affect microbial activity differently compared to lower pressures. An experiment looking at the effect of pressure was performed to see if the H_2 consumption rate changed at higher pressures. Bottles of different initial pressure were used where the H_2 consumption was followed to investigate pressure impact. Laboratory bottles used for the performed experiment had a pressure limitation of 5 barg. Still, only a maximum pressure of around 2 barg was obtained in the bottles due to physical hindrances limiting higher pressure.

16 bottles of 58 mL volume filled with 25 mL medium were used for the pressure experiment. Initial pressures of 100, 500, 1000, and 2000 mbarg were obtained in the bottles and each pressure had duplicates of unsterile and sterile conditions. All the unsterile bottles initially contained the same amount of media, acetate, inoculum, and a gas composition of 90 % H_2 and 10 % CO_2. Acetate and inoculum were added as explained for the growth rate assessment before pressurising the bottles. The sterile bottles only had the media and the gas mix of H_2 and CO_2. Table 3.4 details the bottle setup.

Table 3.4: Experimental bottle setup for the pressure experiment.

Pressure [mbarg]	H_2 % of headspace	CO_2 % of headspace	Medium [mL]	Acetate [µL]	Inoculum [mL]
100	90	10	25	250	2.5
100	90	10	25	250	2.5
500	90	10	25	250	2.5
500	90	10	25	250	2.5
1000	90	10	25	250	2.5
1000	90	10	25	250	2.5
2000	90	10	25	250	2.5
2000	90	10	25	250	2.5
100	sterile 90	10	25	-	-
100	sterile 90	10	25	-	-
500	sterile 90	10	25	-	-
500	sterile 90	10	25	-	-
1000	sterile 90	10	25	-	-
1000	sterile 90	10	25	-	-
2000	sterile 90	10	25	-	-
200	sterile 90	10	25	-	-

To achieve a pressure of 100 mbarg, the gas line method was used, having a gas mix of 90 % H_2 and 10% CO_2 in the line. The bottles were flushed for 1 minute. To obtain 500 mbarg pressure in the bottles, they were flushed like before for 1 min but after 1 minute, the disconnected needle was taken out while gas where still coming into the bottle. The gas line needle was taken out when the CO_2 level was zero (some seconds). The pressure

was measured and adjusted by taking out gas or injecting the gas mix of H_2 and CO_2 using a syringe. 1000 mbarg was achieved in the bottles by first doing the same as for the 500 mbarg bottles, secondly, the syringe method was used to increase the pressure until 1000 mbarg was achieved. The same procedure was followed to obtain 2000 mbarg in the bottles as for the 1000 mbarg bottles.

Experiment 2 was divided into two parts, where the first part started with the bottle set-up shown in Table 3.4. The second part started after almost all the initial pressures of the unsterile bottles decreased to zero and the same bottles was re-pressurized to the same initial pressure as in Part 1. For all the sterile bottles pressure was sampled every sampling day during the whole experiment and the bottles were not re-pressurized like the unsterile bottles.

Part 1
Part 1 lasted for 7 days. Only pressure was sampled for this experiment started at day 0 and was sampled every day (except Day 5 and 6) until the pressure was zero or stopped decreasing. When the pressure was zero, some nitrogen was added to the bottles to obtain overpressure to be able to measure the gas composition using the microGC. Also, pH was measured and liquid samples were taken when the bottles were done for this part. pH and liquid samples were not taken from the sterile bottles at the end of this part.

Part 2
The duration of Part 2 was 9 days and started on day 7 of the total experiment time. The pressure was sampled every day (except Day 12 and 13) until zero or stable pressure was achieved. On day 10, 0.25 mL acetate was added to all bottles to be sure the microbes had good access to acetate. In the end, the gas composition was measured, where N_2 was added to obtain some pressure in the headspace before usage of the microGC if needed. If the bottle pressure were above 1000 mbarg some gas had to be withdrawn using a syringe to be able to use the microGC. Taking out gas was assumed to not change the gas composition in the bottle. pH was sampled for all 16 bottles while liquid samples were taken from the unsterile bottles at the end of this part.

3.2.4 Surface area experiment

In porous storage sites, the contact area of gas and liquid is very big as the reservoir is water wet and the brain will surround the gas in all pores. The main goal of the surface area experiment was to investigate how increasing surface areas was influencing the H_2 consumption. Bottles of varying surface areas were used and the H_2 consumption was followed over time. Some bottles were also stirred to check if constant movements in the liquid increased the H_2 consumption rate. Figure 3.5 shows the bottles and Table 3.5 details the bottle size used for this experiment.

Table 3.5: Details about bottle size used for the surface area experiment.

Diameter [cm]	Radius [cm]	Surface area [cm^2]	Volume [cm^3]
4.24	2.12	14.11	58.35
4.07	2.04	13.00	71.25
5.12	2.56	20.59	117
5.53	2.77	24.01	131.58
8.66	4.33	58.87	579.57

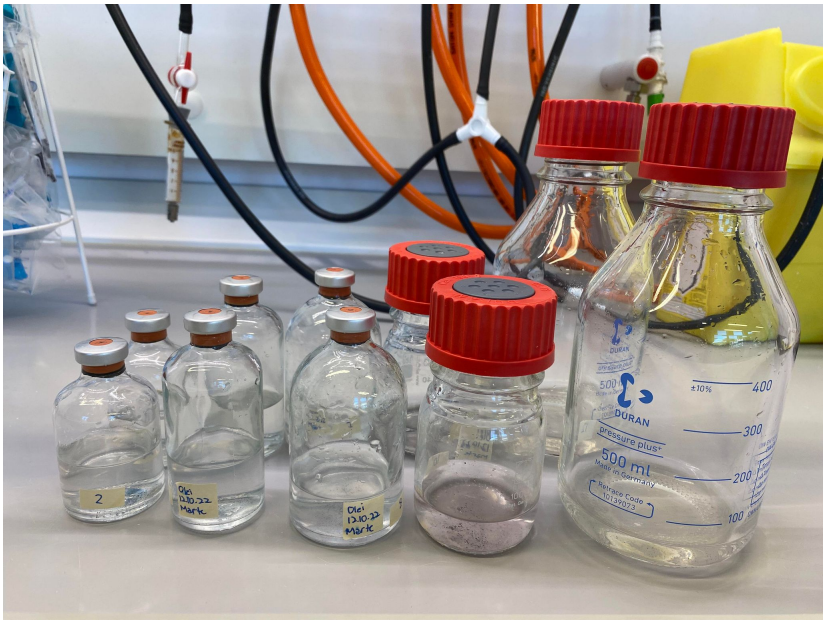

Figure 3.5: Overview of the bottles used for the surface area experiment.

As the media originally was filled in the 58 mL and 117 mL bottles, it had to be moved into the bottles used for this experiment. This was done by opening a bottle and pouring the media over to the wanted bottle before the gas layer was flushed with nitrogen and closed using a stopper and securing it using a crimper or plastic lid. The flushing time varied depending on the volume of the gas layer, where the biggest bottle was flushed for 5 minutes. A burner was on close to the bottles during the whole process to keep the process sterile.

This experiment used 12 bottles where each bottle size had duplicates, and for the 14 cm^2 bottle there were also duplicates using a magnetic stirrer to constantly have liquid movement in the bottle. Sterile bottles were not included in this experiment. All bottles contained the same amount of acetate, inoculum, and a gas mix of 90 % H_2 and 10 % CO_2 and were filled as described for the 90 % bottle in the growth rate assessment. Due to bigger gas volumes for some bottles, the flushing time varied from 1-5 minutes where 5 minutes were used for the biggest bottle. Table 3.6 details the bottle setup. A pressure of around 100 mbarg was kept during the experiment and the procedure of pressurizing

with nitrogen described for the growth assessment was followed. The bottles were stored with the stoppers up for this experiment due to complications of storing them upside down in the incubator.

Table 3.6: Experimental bottle setup for the surface area experiment.

Surface area [cm^2]	H_2 % of headspace	CO_2 % of headspace	Medium [mL]	Acetate [µL]	Inoculum [mL]
14.11	90	10	25	250	2.5
14.11	90	10	25	250	2.5
14.11	90	10	25	250	2.5
14.11	90	10	25	250	2.5
13.00	90	10	25	250	2.5
13.00	90	10	25	250	2.5
20.59	90	10	25	250	2.5
20.59	90	10	25	250	2.5
24.01	90	10	25	250	2.5
24.01	90	10	25	250	2.5
58.87	90	10	25	250	2.5
58.87	90	10	25	250	2.5

The same sampling routine of pH, liquid samples, pressure, and gas composition was performed as for the H_2 concentration experiment. Sampling continued until all H_2 was consumed or the H_2 consumption stopped. After day 7, there was a sampling break due to traveling. This break did not affect the H_2 consumption or the impression of the effect of surface area.

3.2.5 pH experiment

As stated for *Oleidesulfovibrio alaskensis* the growth rate is effected by the pH with a maximum growth pH of 9 [48]. As pH may have a high impact on H_2 consumption, an experiment focusing on the development of pH was performed. Previous experiments indicated a rapid pH increase during the first days. To avoid the pH increase, different concentrations of 3-(N-morpholino)propanesulfonic acid (MOPS) buffers were added to the bottles. MOPS buffer can absorb excess H^+ ions or OH^- ions as it contains a weak acid and its conjugate base meaning it can potentially keep the pH stable [47]. MOPS buffer was supposed to keep the pH more stable and was used to investigate the H_2 consumption rate for different pH developments. Three different MOPS buffer concentrations were used, varying between 1 to 100 mM, as well as having bottles without MOPS buffer, to see how it affects the pH and if the H_2 consumption was acting differently.

12 bottles of 58 mL volume filled with 25 mL medium were used for this experiment. All bottles contain the same amount of medium, acetate, and inoculum as well as the

gas mix of 90 % H_2 and 10 % CO_2. Hence, the bottles included varying amounts and concentrations of MOPS buffer and there were always duplicates of each concentration. MOPS concentrations of 1, 10, and 100 mM MOPS were used in the bottles. Unsterile bottles were not included in this experiment. Table 3.7 details the bottle setup. To get 1 mM MOPS buffer concentration in the bottles, 2.5 mL of a 10 mM MOPS buffer solution was added while 10 mM MOPS buffer concentration was obtained by adding 2.5 mL of a 100 mM MOPS buffer solution. 2.5 mL of a 1 M MOPS buffer was added to get 100 mM concentration in the bottles, while no additional liquid was added for the 0 mM concentrations meaning the liquid volume in the bottles was lower than the others. Three lactate bottles, one for each concentration, were included in this experiment to check if the MOPS buffer was toxic to the microbes.

Table 3.7: Experimental bottle setup for the pH experiment.

MOPS buffer [mM]	H_2 % of headspace	CO_2 % of headspace	Media [mL]	Acetate [µL]	Inoculum [mL]	Lactate [mL]
0	90	10	25	250	2.5	-
0	90	10	25	250	2.5	-
1	90	10	25	250	2.5	-
1	90	10	25	250	2.5	-
10	90	10	25	250	2.5	-
10	90	10	25	250	2.5	-
100	90	10	25	250	2.5	-
100	90	10	25	250	2.5	-
1	0	0	25	-	2.5	600
10	0	0	25	-	2.5	600
100	0	0	25	-	2.5	600

The sampling routine for the pH experiment was mostly the same as for the H_2 concentration experiment but differs for the pH sampling. As pH is the main focus of the experiment the pH was sampled every sampling day. This experiment lasted for 63 days and was divided into three parts as the bottles were re-filled with H_2 twice during the experiment. The sampling was performed almost daily for the first part, but less frequently for Part 2 and 3 due to slower H_2 consumption rates. The pressure was held at around 100 mbarg and the procedure of adding N_2 to increase pressure was following as for previous experiments.

Part 1

The first part lasted for eight days, where the bottles were sampled according to the sampling routine until the microbes consumed all available H_2, or the amount of H_2 in the headspace was very small. Liquid samples were taken after Part 1.

Part 2

The second part of the experiment lasted for 20 days, including 12 sampling days. The bottles was sampled according to the sampling routine until the bottles almost consumed all the H_2. On day 10, 0.25 mL acetate was added to all the bottles to make sure the access to acetate was not a limiting factor for H_2 consumption. Also, MOPS buffer was added to the 10 and 100 mM MOPS bottles with the same initial concentrations, with the intention to lower the pH. On day 16, sulfate was added to all bottles to get 30 mM sulfate in the bottles. Access to sulfate is required for microbial growth of this strain and was added to be sure sulfate was not a limiting factor for H_2 consumption. At day 21, 2.5 mL of the 1 M MOPS buffer was added to all the bottles, except the 100 mM MOPS bottles, to obtain 100 mM MOPS in the bottles. A MOPS buffer of higher concentration was added on day 21, as the lower concentration MOPS buffers added on day 10 had low effect of decreasing the pH in the bottles. Liquid samples were not taken at the end of this part.

Part 3

The duration of the third part was 28 days, including six sampling days. The bottle was sampled according to the sampling routine until all H_2 was consumed, or until the experiment was stopped. At day 35 both acetate and sulfate were added with the same concentration as previously to make sure microbial growth was not limited due to access to sulfate or acetate. Liquid samples were taken at the end of the experiment.

3.3 Calculations

This section provides an overview of the calculations used for analysing data, and the sensitivity of the collected data is described.

H_2 acts like an ideal gas at very low pressure [53], and as a maximum pressure of 2 bar was used in the bottles, the ideal gas law (Equation 3.2) can be used to calculate number of moles (n) of H_2 in the bottles. R is the gas constant at 8.31 $m^3PaK^{-1}mol^{-1}$ and for all experiments, the temperature (T) was 37 °C (310 K). By knowing the volume of the gas layer (V_g) in m^3, gas composition data were used to calculate the volume of headspace taken by H_2 (V_{H_2}) in m^3, shown by Equation 3.1. Pressure (P) is equal to the measured bottle pressure plus atmospheric pressure. Examples of raw data of pressure and gas composition used in the ideal gas law can be found in Appendix B.

$$V_{H_2} = \frac{V_g \cdot Prosentage_{H_2}}{100} \tag{3.1}$$

$$PV = nRT \tag{3.2}$$

The daily consumption rate was calculated using Equation 3.3. x_1 and x_2 refer to the sampling day while y_2 and y_1 is the H_2 consumed for these days.

$$Maximum\ consumption\ rate = \frac{y_2 - y_1}{x_2 - x_1} \tag{3.3}$$

Equation 3.4 was used to calculate the unknown volume when diluting a solution in another solution. C_1 and V_1 refer to the initial concentration and volume of the solution in mM and mL while C_2 and V_2 is the final values with the same units. This equation was used when adding sulfate and MOPS buffer to the bottles.

$$c_1 \cdot V_1 = c_2 \cdot V_2 \tag{3.4}$$

3.3.1 Sensitivity

The collected data and calculates include some uncertainty and sensitivity that may effect the results and will be described in this section.

As both the gas transducer and the GC measurement take out gas samples during sampling, gas was lost during the experiment. To be able to see the actual H_2 consumption rates, this loss had to be subtracted from the H_2 consumption. To calculate sampling loss, pressure was sampled both at the beginning and at the end of the daily sampling. By calculating how much H_2 there was in the bottles, using the ideal gas law, at the beginning of the daily sampling, using the start pressure, and how much H_2 there was at the end of the sampling using the end pressure, it was possible to calculate the loss of H_2 by looking at the difference of the numbers of moles. For all graphs (except the pressure experiment) showing the H_2 consumption in the Result chapter, includes this loss in order to focus on the microbial H_2 consumption.

During the experiment, the bottles were stored in the incubator at 37 °C but temporarily removed during sampling. Depending on the sampling time, the temperature may decrease in the bottles. A temperature decrease will affect the sampled bottle pressure, which again will affect the calculated number of mmoles using the ideal gas law. This may cause some errors in the graphs.

The pH meter used to measure the pH of bottle samples for most experiments, seemed to be sensitive to salinity, meaning the pH meter worked more accurately when measuring high-salty solutions. As Medium 195c was of low salt, a error between the sampled value and the real value was observed. This error was estimated before pH sampling using a pH 7 buffer where the difference between the sampled value for the pH 7 buffer and the known value of 7 was used as an error for all sampled values. A new pH meter started to

be used in the middle of the pH experiment (the last performed experiment), where this error was disregarded.

The importance of this study was to investigate the behavior of *Oleidesulfovibrio alaskensis* and how it consumed H_2. As microbes are living beings, they can grow differently under the same conditions. For this reason, duplicates were used to notice any variations of microbial H_2 consumption. The presented data shows the average of the duplicates and includes error bars to visualise the deviation between H_2 consumption of the duplicates. The error bars were calculated using average deviation. The average was calculated using Equation 3.5 and the average deviation by Equation 3.6 where $\overline{x}$ is the average value, x_i is the data values in the given set and n is the total number of data values. Calculations performed for this study do not include uncertainty. Variation of H_2 consumption between the duplicates and observing trends in the H_2 consumption was of higher importance than the measurement uncertainty of equipment and instrument at this stage of the research on this topic and therefore not paid attention to in this study.

$$\overline{x} = \frac{1}{n}\sum_{i=1}^{n} x_i = \frac{1}{n}\left(x_1 + \cdots + x_n\right) \tag{3.5}$$

$$Average\ Deviation = \frac{1}{n}\sum_{i=1}^{n} |x_i - \overline{x}| \tag{3.6}$$

Some experiments included sterile control bottles to prove that other chemical reactions were not affecting the H_2 in the bottles or if the experimental conditions had unexpected effects. The surface area and pH experiments did not include sterile control bottles as the two previous experiments did not prove any significant observations and also for saving time during sampling.

The start pH of the bottles was assumed to be similar as the media initially had the same pH. Therefore, the pH of three or four bottles was measured on Day 0, where the average of those bottles was assumed to be the pH of all bottles. The average was calculated using equation 3.5. The error bars were calculated as standard deviation (Equation 3.7).

$$Standard\ Deviation = \frac{1}{n}\sum_{i=1}^{n} |x_i - \overline{x}| \tag{3.7}$$

The microGC had high uncertainty related to the H_2S measured in the gas composition. The microGC was only calibrated up to 1 % of H_2S, meaning that values above 1 % include high uncertainty.

Chapter 4

Results and discussion

This chapter will present the experimental results of bottle experiments focusing on H_2 consumption and microbial behavior related to the microbial strain *Oleidesulfovibrio alaskensis*. The results will be discussed with a focus on how factors like concentration, pressure, surface area, and pH affect the H_2 consumption rates. These factors are highly relevant for gas reservoirs and such data is needed to understand the impact of this strain before implementing UHS technology. In the end, the results from the bottle experiment will be compared to a microfluidic experiment to notice if the trends observed in the bottles relate to the behavior in the porous media.

4.1 Growth rate assessment

To assess the growth rate of *Oleidesulfovibrio alaskensis* one bottle containing 10 % H_2 and one with 90 % H_2 in the headspace was used, where H_2 consumption was followed for four days. Sampling was performed daily to follow the consumption rate, and the result is presented in Figure 4.1. For the 10 % H_2 bottle all H_2 was consumed after two days and the maximum consumption rate was observed from Day 1 to Day 2. The 90 % H_2 bottle consumed almost all the H_2 during four days, but was assumed to finish the next one to two days based on the consumption rate. The sampling stopped after four days, even if one bottle still had H_2 left, as the impression of the microbial growth rate was clear.

pH was sampled to get some insight into how *Oleidesulfovibrio alaskensis* affect the pH. Table 4.1 shows the pH sampled at Day 0 and the day all H_2 were consumed or sampling stopped. For the 10 % H_2 bottle, a small pH increase was observed, while a higher pH increase was seen for the 90 % H_2 bottle. This indicates a rapid pH increase for this strain in contact with H_2.

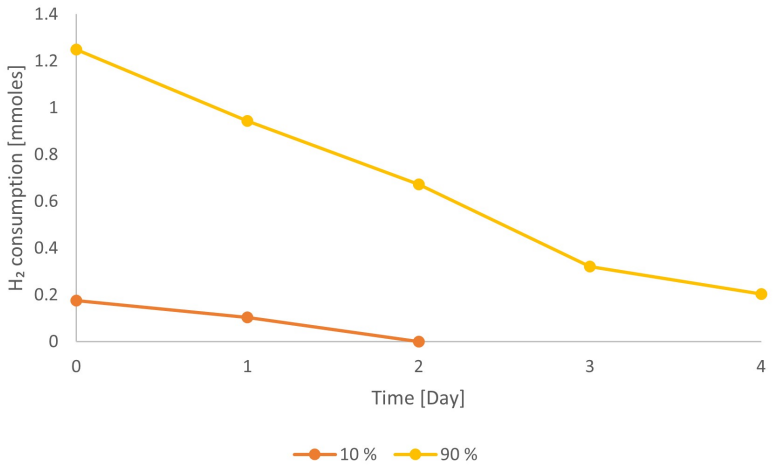

Figure 4.1: H_2 consumption for growth rate assessment

Table 4.1: pH for growth rate assessment.

Bottle	pH (Day 0)	pH (end)
10 %	8.0	8.1
90 %	7.4	9.3

By only using two bottles, the growth rate of this strain was clear, and decisions on a sampling routine for future experiments could be considered. As the 10 % H_2 bottle consumed all the H_2 after two days and the 90 % H_2 bottle almost consumed all the H_2 during four days, a sampling procedure of daily sampling seemed necessary for upcoming experiments. As the main goal of this experiment was to assess the growth rate, no duplicates were used.

4.2 Hydrogen concentration experiment

Bottles of initial 0, 10, 40, and 90 % H_2 were used, and H_2 consumption was followed daily to investigate the more suitable gas mixture for UHS. The 0 % bottle was included in this experiment to see if there were any unexpected chemical reactions for the microbes, but will not be shown in the H_2 consumption figures as there is no H_2 in the bottles. Sterile bottles having the same initial concentration of H_2 were included in this experiment to notice any unpredictable chemical reactions appearing at the conditions set for the experiment.

Figure 4.2 shows the H_2 consumption represented as headspace H_2 content in millimoles (mmoles) over time. The solid lines show the unsterile bottles where different colors represent the different H_2 concentrations while the sterile bottles are given by the dotted lines corresponding with the same color. As the graphs show, all unsterile bottles consume

all the H_2 over seven days, where the lower concentration bottles consumed all H_2 first. Higher daily consumption rates were observed during the first days for the 40 and 90 % H_2 concentrations, while the daily consumption rate was lower in the end. The graphs representing the sterile bottles were slightly decreasing, most visible for the sterile 90 % graph. As there were no microbes consuming H_2 and the graphs included sampling loss, the H_2 amount was expected to be the same during the whole experiment. This loss of H_2 can be related to gas escape through the stoppers (top of the bottle) or sampling error. These loss mechanisms also occur in the unsterile bottles, leading to lower H_2 microbial consumption than stated. As the graph shows, this H_2 loss is small and does not affect the main outcome of this experiment. The error bar represents the average deviation for the duplicates and indicates differences in H_2 consumption for the two bottles. Some error bars are more visible than others but all duplicates were mostly following the same trend for consuming H_2. Some error bars are too small to be seen in the figure.

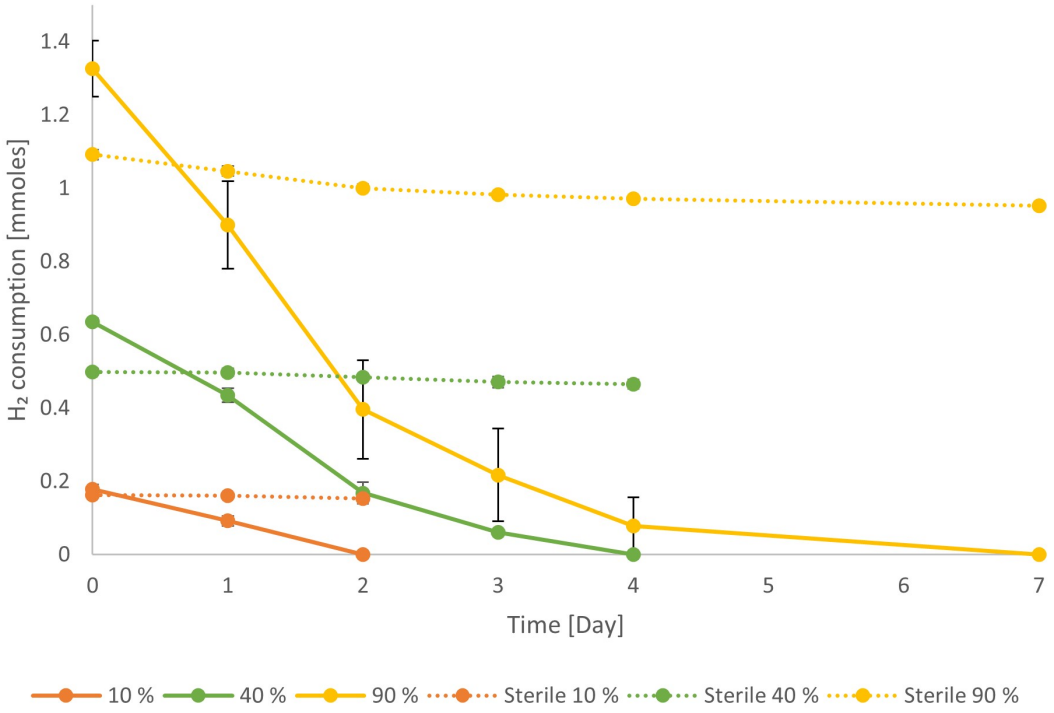

Figure 4.2: H_2 consumption in mmoles where initial concentrations of H_2 vary from 0 to 90 %. Straight lines represent unsterile bottles, while dotted lines show the sterile bottles. Error bars represent the average deviation between the duplicates and tell if the duplicates grow differently.

Relative H_2 consumption for each concentration can be seen in Figure 4.3. Solid lines represent bottles with microbes while dotted lines are sterile bottles. As the figure shows, the 40 and 90 % H_2 concentrations followed the same trend while the 10 % H_2 concentration differed. The relative H_2 consumption rate was higher for the 10 % H_2 concentration

meaning the available H_2 was consumed faster compared to the other bottles. Again, the sterile graphs show some H_2 consumption indicating some loss of H_2.

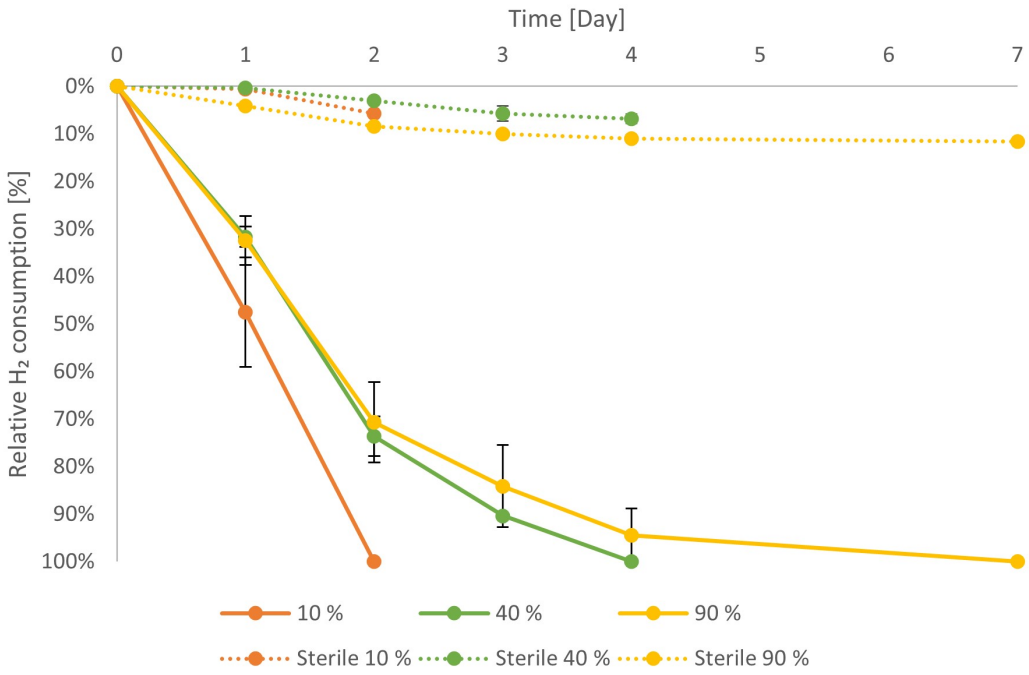

Figure 4.3: Relative H_2 consumption in percentage where initial H_2 concentrations of 10, 40 and 90 % is represented. The average deviation is represented as the black error bars.

Table 4.2 gives the start and end pH values as well as the maximum consumption rate per day in mmoles/day and total H_2 consumption in mmoles. Based on the literature a pH increase was expected for the unsterile H_2 containing bottles [45], while stable pH was expected for the other bottles. The pH was stable for the 0 % H_2 concentration as there was no H_2 present to affect the pH. A small pH increase was observed for the 10 % H_2 concentration from start to end, while a higher pH increase appeared for the 40 and 90 % H_2 concentrations. For the 90 % H_2 concentration the pH approached the maximum growth pH at 9. Based on the data, the pH increase seems to correspond to the access to H_2, where more H_2 gives a higher pH increase, and the pH is increasing to the maximum growth pH when access to H_2 is unlimited. The pH increase for this experiment was similar to the observation done for the growth rate assessment.

The daily consumption rate in mmoles was calculated for each day and the maximum consumption rate is presented in Table 4.2. Calculations show higher maximum consumption rate correlates to higher initial H_2 concentrations. Mostly, the maximum consumption rate appeared from day 1 to 2, except for one of the 10 % H_2 bottles that appeared from day 0 to 1. The maximum consumption rate tells that the microbes are more active from day 1 to day 2 and they consume more H_2 per day when there is more H_2 available.

For all H_2 concentrations, the H_2 was completely consumed, and the total amount of consumed H_2 was higher for higher concentrations as there were more H_2 available.

Table 4.2: Start and end pH, maximum consumption rate, and total H_2 consumption are given for each concentration used for this experiment. It is assumed that the start pH is the same for all bottles. Therefore, the pH was sampled for three bottles at day 0 and the average value including uncertainty is used for all bottles.

Bottle	pH (Day 0)	pH (Day 7)	Maximum consumption rate [mmoles/day]	Total H_2 consumption [mmoles]
0 %	7.2 ± 0.1	7.2 ± 0.1	-	-
10 %	7.2 ± 0.1	7.3 ± 0.0	0.11 ± 0.00	0.18 ± 0.01
40 %	7.2 ± 0.1	8.2 ± 0.0	0.27 ± 0.01	0.64 ± 0.01
90 %	7.2 ± 0.1	8.9 ± 0.2	0.50 ± 0.01	1.33 ± 0.08
Sterile10 %	7.2 ± 0.1	7.0 ± 0.0	0.01 ± 0.00	0.01 ± 0.00
Sterile40 %	7.2 ± 0.1	7.3 ± 0.0	0.01 ± 0.00	0.03 ± 0.00
Sterile90 %	7.2 ± 0.1	7.3 ± 0.1	0.05 ± 0.00	0.13 ± 0.00

Figure 4.4 shows the headspace H_2S content in mmoles over time. For most of the unsterile bottles, an increase of the H_2S content was observed in the first four days, with some variations, before it stopped or decrease on Day 7. The amount of H_2S gas increases in the first days as HS^- is produced (see SRB reaction in Table 2.2). As explained earlier, H_2S will be present as HS^- in liquid and as H_2S when it appears as a gas. The balance between H_2S as a gas and HS^- dissolved in liquid follows the Bjerrum plot (see Figure 2.3) depending on the pH. During the first days of the experiment, some of the produced HS^- was converted to H_2S as the pH started at 7.1, and a H_2S increase was observed. As the pH increased over time, the fraction of H_2S. (thats the reson) goes down and may be the reason for the H_2S decrease in the end. Also, (assume)the HS^- production slowed down as the H_2 consumption rates were lower. As H_2S is toxic and pure H_2 is favorable when withdrawing the stored gas, the pH increase is beneficial. For some of the data points, large error bars can be observed. The uncertainty related to the H_2S percentage measured using the microGC is high when the value is over 1 % (see Section 3.2.7). Therefore, there was high uncertainty related to these values. Nevertheless, the trend of increasing H_2S in the beginning and decreasing on the last day agrees well with the literature and is assumed to be correct.

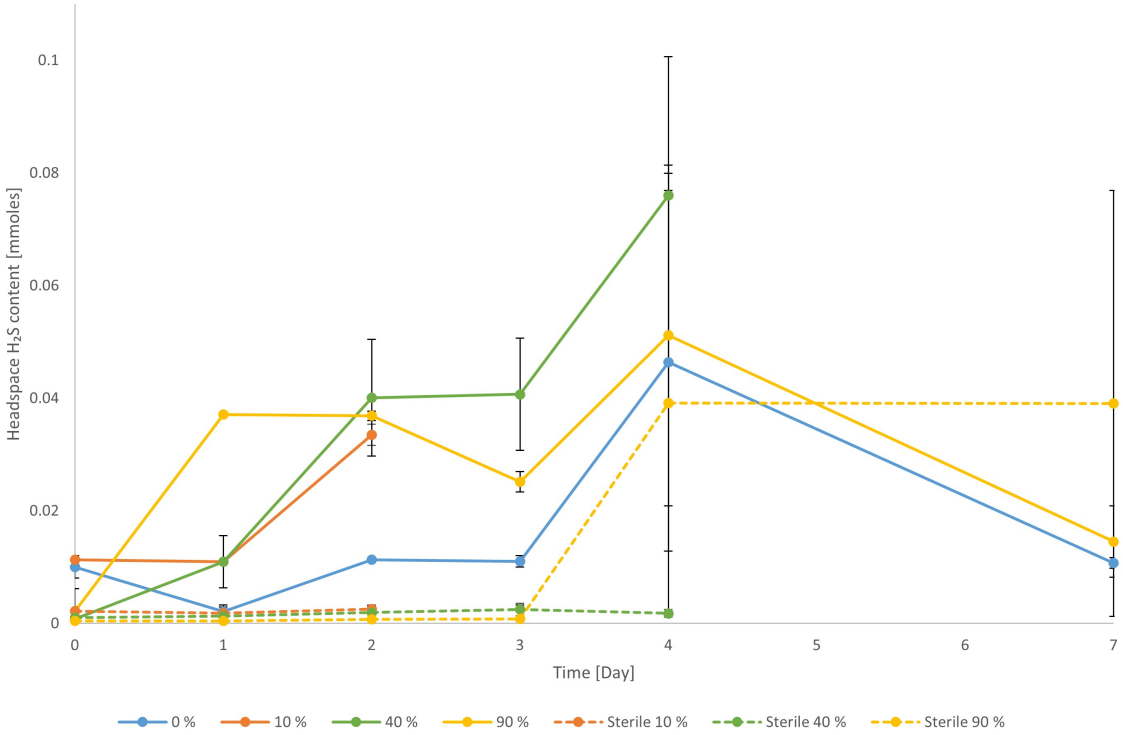

Figure 4.4: H_2S content in the headspace over time for each concentration. The variation of H_2S is due to production but also dependent on the pH.

The acetate concentration was measured at day 0 and at the end of the experiment to investigate how *Oleidesulfovibrio alaskansis* is consuming acetate. As acetate is a carbon source, described to be consumed by the strain, acetate could potentially be a limiting factor for microbial activity. Only samples of two bottles were measured at day 0, where the average of those is assumed to be similar to the concentration of all bottles on day 0 as the same amount of acetate was added to all bottles. In the end, the acetate concentration of the 10, 40, and 90 % H_2 bottles was measured. The average acetate concentration including the average deviation is shown in Table 4.3. The end concentration for each H_2 concentration was not significantly differing from the initial acetate concentration, indicating that the microbes are not consuming or producing acetate. Based on the acetate concentration data for the performed experiment, access did not limit the H_2 consumption.

Table 4.3: Acetate concentration in mg/L for some of the bottles at the beginning and at the end of the experiment. Samples of two bottles were used to calculate the acetate concentration at day 0.

	Acetate [mg/L]
Day 0	1218 ± 22
10 % (end)	1169 ± 10
40 % (end)	1127 ± 29
90 % (end)	1182 ± 19

It is long known that SRB grows on consuming H_2 [33], which *Oleidesulfovibrio alaskensis* also do, based on the results. Figure 4.3 shows that the relative H_2 consumption rates were different for the different gas mixtures. Based on the results gas mixture of higher H_2 % is better for this strain as the relative H_2 consumption is higher for the 10 % H_2 concentration. Anyways, the differences in relative consumption rates were not significantly large and all H_2 was consumed in the end.

4.3 Pressure experiment

Bottles of initial gauge pressure ranging from 100 to 2000 mbarg were used, and (almost) daily sampling was performed to follow the H_2 consumption for the different pressures. The bottles were re-pressurized to the same initial pressure on day 7 to see if the consumption appeared similar or if the consumption slowed down. However, the pressure used for this experiment was relatively low compared to reservoir pressure due to pressure limitations for the laboratory bottles at 5 bar and the bottles were pressurized manually. Anyway, the pressure experiment was expected to give an impression of how higher pressure impact H_2 consumption.

Figure 4.5 shows the pressure development for both Part 1 and 2 of the experiment. The graphs do not include sampling loss as only pressure was measured in the daily sampling routine. Unsterile bottles are represented as solid lines, while dotted lines present the sterile bottles, where the same color is used for the same pressure for both sterile and unsterile bottles. As the graphs show the initial pressure was higher than the specified value for the unsterile bottles, due to injection of acetate and inoculum after adjusting the pressure. Added liquid volume of 2.8 mL, increased the pressure above the specified values before the experimental start. As the graphs do not include sampling loss, the sterile graphs were decreasing. As sample loss could not be calculated for this experiment, the unsterile and sterile graphs were compared to see if the pressure reduction was only due to sampling loss or if H_2 was consumed. During Part 1, all unsterile graphs except the 2000 mbarg graphs went to zero mbarg where higher initial pressure lasted longer before they reached zero pressure. The error bars associated with the 2000 mbarg graph for Part

1 were larger compared to other pressures, indicating variations in the growth between the duplicates. Actually, one of the 2000 mbarg bottles had zero pressure on day 7 while the other still had 530 mbarg. The pressure difference may be explained by microbes acting differently, some extra microbial cells in one bottle, or just more optimal conditions for growth. On day 7 the bottles were re-pressurized to the same initial pressure, but as the graphs show, the pressure rate slowed down compared to the first part indicating lower H_2 consumption rates. The 100 mbarg graph was the only pressure going to zero in Part 2. The 500 and 1000 mbarg bottles consumed some H_2 during the first two days of Part 2 before the H_2 consumption slows down or stops completely. After day 10 the sterile and the unsterile graphs for the 500 and 1000 mbarg bottles almost follow the same trend indicating the loss of pressure is due to sampling loss and not H_2 consumption. The 2000 mbarg graphs for sterile and unsterile bottles almost follow the same trend during part 2 indicating zero H_2 consumption.

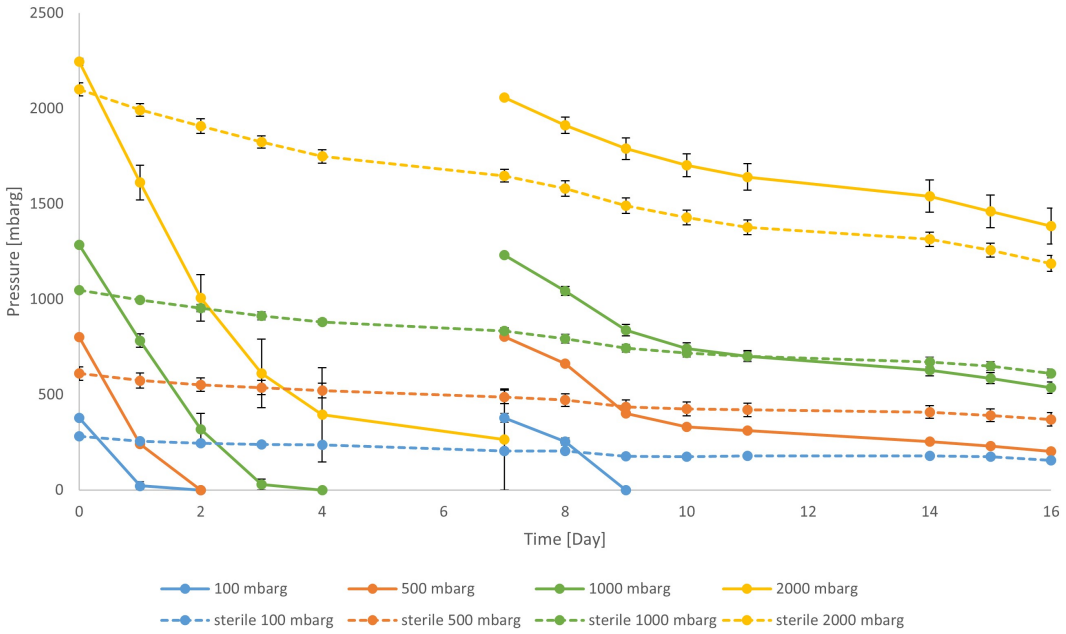

Figure 4.5: Pressure development in mbarg where initial pressure varies from 100 to 2000 mbarg. Straight lines represent unsterile bottles, while dotted lines follow the sterile bottles. Error bare is included for all data points and tells how the duplicates were growing relative to each other.

The relative H_2 consumption is shown in Figure 4.6 where the solid lines represent the unsterile bottles for Part 1, while the dotted lines represent the unsterile bottles for Part 2. In this Figure, the Part 2 graphs start at day 0 to easily compare the graphs. Unsterile bottles were not included in this figure. During the first part, the 100 and 500 mbarg graphs followed the same trend and had a higher relative consumption rate compared to the 1000 and 2000 mbarg graphs. Also, the 1000 and 2000 mbarg graphs followed the same trend the first days before they differed where the 2000 mbarg graph slowed down.

For Part 2, the relative consumption graphs acted the same as the pressure graphs as the consumption stopped for some of the bottles.

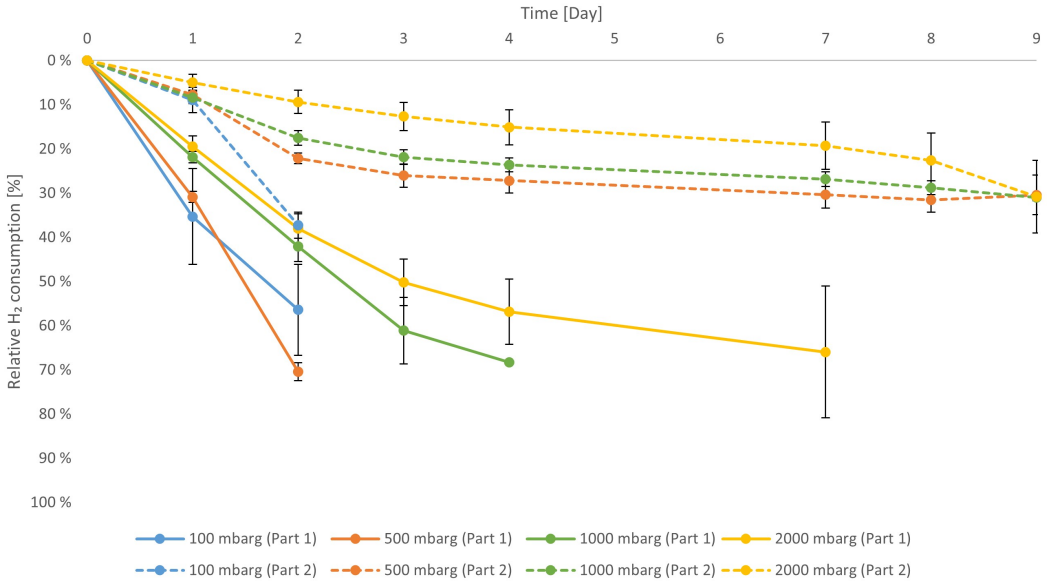

Figure 4.6: Relative H_2 consumption in percentage where initial pressure of 100, 500, 1000, and 2000 is represented. The average deviation is represented as the black error bars.

As the bottles were pressurized before adding acetate and inoculum, pH was not feasible to measure at day 0 and was only measured at the end of each part. The start pH was assumed to be similar to the concentration experiment as the same media batch and the same solutions were added. For the sterile bottles, the pH was only sampled at the end of the experiment due to the high pressure of some of the bottles after Part 1. pH values are presented in Table 4.4. As the pH was assumed to be around 7.2 at day 0, a pH increase occurred during Part 1. The H_2 consumption in mmoles for Part 1 was related to the initial pressure, where higher initial pressure gave a higher H_2 consumption (see Figure 4.7), and a higher pH increase was therefore expected for the higher pressure. As the pH values for Part 1 show, this was consistent for the 100, 500, and 1000 mbarg, while the pH value for the 2000 mbarg was between the value for the 100 and 500 mbarg. The pH may have been affected by higher pressure or the deviation was due to sampling mistakes (human error). The end pH shows a small increase for all pressures where the pH ends up at the same value of 8.8, except for the 1000 mbarg, where a decrease in pH was observed. Sampling mistakes may explain this deviation. For this experiment, the pH did not reach the maximum growth pH and was assumed not to stop the H_2 consumption. By assuming the start pH to be 7.2, a pH increase of 0.2 to 0.7 was observed for the sterile bottles. This pH increase was higher compared to the sterile bottles in the concentration experiment, where the pH was stable or increased by 0.1. The development and impact

of pH were investigated in the pH experiment and discussed in more detail below.

Table 4.4: pH after Part 1 and 2 and maximum consumption rate is given for each pressure bottle used for this experiment. It is assumed that the pH at day 0 is the same (7.2) as for the concentration experiment.

Bottle	pH (Day 7)	pH (Day 16)	Maximum consumption rate [mmoles/day] (Part 1)	Maximum consumption rate [mmoles/day] (Part 2)
100 mbarg	8.5 ± 0.0	8.8 ± 0.1	0.66 ± 0.03	0.42 ± 0.01
500 mbarg	8.7 ± 0.1	8.8 ± 0.1	0.77 ± 0.01	0.28 ± 0.00
1000 mbarg	8.8 ± 0.2	8.6 ± 0.1	0.54 ± 0.03	0.22 ± 0.01
2000 mbarg	8.6 ± 0.0	8.8 ± 0.0	0.68 ± 0.07	0.16 ± 0.05
Sterile100 mbarg	-	7.4 ± 0.0	0.03 ± 0.00	0.03 ± 0.00
Sterile500 mbarg	-	7.8 ± 0.0	0.04 ± 0.00	0.04 ± 0.00
Sterile1000 mbarg	-	7.9 ± 0.0	0.05 ± 0.00	0.05 ± 0.00
Sterile2000 mbarg	-	7.9 ± 0.0	0.12 ± 0.00	0.10 ± 0.00

The maximum consumption rate in mmoles per day was calculated and is presented in Table 4.4. For Part 1 a higher maximum consumption rate was observed for the 500 mbarg compared to the others, while the lowest rate was calculated for the 1000 mbarg. The maximum consumption rate was similar for the 100 mbarg and 2000 mbarg. For Part 2, the maximum consumption rate was higher for the 100 mbarg compared to the other bottles. As the H_2 consumption stopped in the beginning or during the second part for all pressures except the 100 mbarg, higher values were expected for the 100 mbarg.

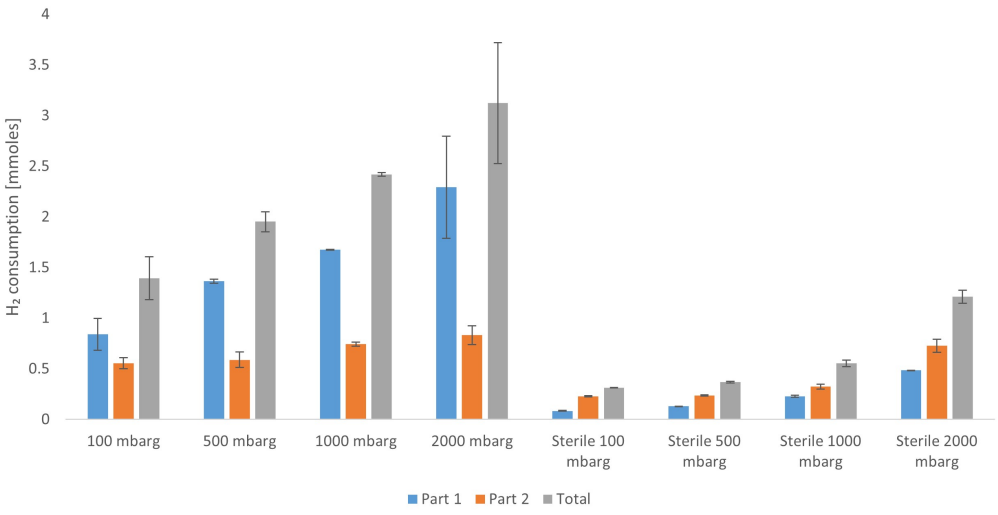

Figure 4.7: H_2 consumption for Part 1 (blue), part 2 (orange), and total H_2 consumption (grey).

Also for this experiment, the concentration of acetate was measured, but only at the end

of the experiment (see Table 4.5). The acetate concentration at day 0 was assumed to be the same as for the concentration experiment as the same amount was added. As knowledge of acetate consumption was not investigated at this point (was investigated after all experiments were performed), acetate was added on day 10 of the experiment to make sure good availability of energy source for the microbes. As explained for the concentration experiment, *Oleidesulfovibrio alaskensis* did not consume any acetate, and as the acetate was added with the same amount as initially the concentration measured in the end was approximately doubled.

Table 4.5: Acetate concentration in mg/L for some of the bottles at the end of the experiment.

	Acetate [mg/L]
500 mabr	2160 ± 53
1000 mbar	2256 ± 46
2000 mbar	2467 ± 309

The solubility of H_2 is defined to be low in water [23], but higher pressure may increase the solubility. Osman *et al.* investigated the impact of pressure on H_2 solubility in water and brine showing a higher solubility with increasing pressure. As the microbes consume the H_2 on the gas-liquid interface or H_2 dissolved in the media, a higher maximum consumption rate was expected for the higher-pressure bottles as more H_2 may be dissolved and could potentially be consumed similarly. As the maximum consumption rate for Part 1 indicates, increasing solubility with increasing pressure was not consistent with the observations. The higher solubility may not occur as low pressure was used for this experiment.

As Figure 4.5 show the H_2 consumption stopped during the second part for most bottles. For microbial growth certain conditions must be fulfilled for this strain, like access to carbon sources, a specific range of pH, and access to sulfate [17, 48]. As Table 4.4 presents, the pH is within the growth pH range stated for this strain and was assumed to not stop the H_2 consumption. As Table 4.5 shows and explained above, the microbes were not consuming the acetate, and the availability of acetate was not a limiting factor for microbial growth. Access to sulfate is also a key factor for microbial growth. Calculations for sulfate reduction (see Appendix D.1) tells us that 2.1 mmoles of H_2 can be consumed before the initial amount of sulfate runs out in the experimental bottle used for this experiment. The 2000 mbarg pressure had a total H_2 consumption of 2.3 mmoles H_2 during part 1 (see Figure 4.7). No access to sulfate can be assumed to explain the stop in H_2 consumption for these bottles for Part 2 and can even explain why one of the bottles stopped consuming at the end of Part 1. The 1000 mbarg pressure reached a H_2 consumption of 2.1 mmoles H_2 during Part 2 and is assumed to explain the stop in

H_2 consumption. The 500 mbarg pressure was only consuming 1.9 mmoles H_2 during the whole experiment and can not directly explain why the microbial growth stopped, and further investigation is needed to understand the reason for zero H_2 consumption in the end. The 100 mbarg pressure never stopped consuming during the experiment, so limiting access to sulfate was not a problem for these bottles.

4.4 Surface area experiment

Bottles of different surface areas ranging from 13 to 58 cm^2 were used and H_2 consumption was followed to investigate the impact of increasing contact area of liquid and gas. Also, this experiment investigated the impact of having constant movement in the liquid phase focusing on how it affects the consumption rate.

Figure 4.8 shows the relative H_2 consumption as a percentage of the initial amount of H_2. As the graphs show, the bottles of surface area 21, 24, and 59 cm^2 did not consume all the H_2 while the smaller bottles of 13 and 14 cm^2 consumed all the H_2. The relative consumption rate was higher for the stirred 14 cm^2 bottle and finished first, compared to the other 14 cm^2 bottles and the 13 cm^2 bottles finish later on. Sampling between Day 7 and 24 did not occur (due to traveling), but as the 14 cm^2 graph was closer to zero on Day 7 it was assumed that these bottles consumed all the H_2 before the 13 cm^2 bottles. The relative H_2 consumption was observed to almost follow the same trend for the 14 and 13 cm^2 graphs the first three days before the graphs differ significantly. The 21 and 24 cm^2 graphs follow the same trend, but differ some in the end. As the error bar is overlapping the difference may be explained by more optimal growth conditions in some of the bottles causing some differences in microbial activity. The relative consumption rate for the 59 cm^2 bottles was much lower compared to the other bottles. The data point of day 1 is not possible to see in the Figure as the calculation gave negative H_2 consumption. This is not possible and may be due to temperature loss during sampling causing wrong calculations using the ideal gas law.

As for the concentration experiment, pH was sampled for four bottles at Day 0, and the average of those bottles was assumed to be the pH for all bottles at Day 0. pH for Day 0 and the end pH are presented in Table 4.6. The pH measured on Day 0 was higher compared to the Day 0 pH measured for the H_2 concentration experiment. This may be due to the new media batch used for this experiment. The presented values show a pH increase up to around 9, which is defined as the maximum growth pH [48]. The end pH for the 21 and 24 cm^2 bottles was 9.2, which may explain why the H_2 consumption stopped. For the 59 cm^2 bottles the pH reached 8.7 and can not directly explain the zero H_2 consumption, but as the pH is not optimal it can be a factor affecting the decrease in H_2 consumption rate.

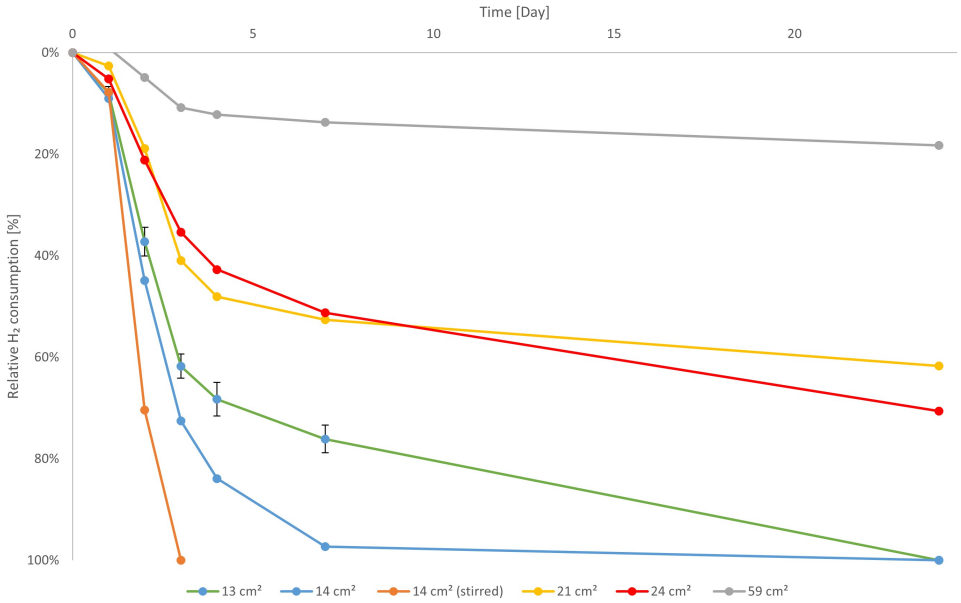

Figure 4.8: Relative H_2 consumption

The maximum consumption rate in mmoles per day is presented in Table 4.6. The magnetic stirrer was inserted to check if movement in the liquid increased the solubility of H_2 in the liquid. Higher solubility of H_2 was expected to give higher maximum consumption rates as more H_2 could be consumed simultaneously. As the maximum consumption rate for the 14 cm^2 stirred bottles was double the size compared with the static condition it seems to be consistent with the hypothesis. Also, it was expected to see a higher maximum consumption rate for larger surface areas as more H_2 is in contact with the bacteria. This was not consistent as the 13 cm^2 bottles and the 24 cm^2 bottles had almost the same maximum consumption rate, and the 13 cm^2 bottle had a higher maximum consumption rate than the not stirred 14 cm^2 bottles.

Table 4.6: Start and end pH, maximum consumption rate, and total H_2 consumption are given for each bottle size used for this experiment. It is assumed that the start pH is the same for all bottles. Therefore, the pH was sampled for four bottles at day 0 and the average value including uncertainty is used for all bottles.

Bottle	ph (Day 0)	pH (End)	Maximum consumption rate [mmoles/day]	Total H_2 consumption [mmoles]
13 cm^2	7.7 ± 0.0	8.9 ± 0.0	0.54 ± 0.01	1.84 ± 0.03
14 cm^2	7.7 ± 0.0	9.0 ± 0.2	0.41 ± 0.02	1.16 ± 0.10
14 cm^2 stirred	7.7 ± 0.0	9.0 ± 0.0	0.78 ± 0.13	1.24 ± 0.01
21 cm^2	7.7 ± 0.0	9.2 ± 0.0	0.85 ± 0.05	2.38 ± 0.10
24 cm^2	7.7 ± 0.0	9.2 ± 0.0	0.53 ± 0.08	2.32 ± 0.08
59 cm^2	7.7 ± 0.0	8.7 ± 0.0	1.35 ± 0.48	3.81 ± 1.47

The total H_2 consumed in mmoles is presented in Table 4.6. As the 13, 14, and 14 cm^2 stirred consumed all the H_2, the total H_2 consumed in mmoles relates to the available gas volume. The gas volume for the 13 cm^2 bottles was bigger compared to the 14 cm^2 bottles and gives a higher total H_2 consumption. For the 14 cm^2 bottles (static and stirred), the total H_2 consumption was expected to be the same, but small differences were observed and may be explained by small variations of initial media volume or the volume of the magnet occupying some of the potential gas volumes. As explained for the pressure experiment, 2.1 mmoles of H_2 can be consumed before all the initial amount of sulfate was consumed. As the total H_2 consumption was above this value for the 21, 24, and 59 cm^2 bottles, the access to sulfate can be the limiting factor for continued consumption of H_2. For the 59 cm^2 bottles a H_2 consumption of 3.8 mmoles was observed including a deviation of 1.4 mmoles. Looking at the total H_2 consumption for each duplicate the consumption was at 2.3 mmoles for one of the bottles and 5.3 mmoles for the other bottle. For the duplicates of 59 cm^2 bottles different stoppers were used to close the bottles, where the tightness of the stoppers may differ. A less tight stopper will cause gas leakage and may explain the high total consumption value of 5.3 mmoles. Also, a total H_2 consumption 2.2 mmoles above the value where it is assumed the bottles run out of sulfate seems unpredictable and is assumed to be wrong. Different stoppers were used due to indications of oxygen in one bottle before the experimental start. It was assumed that the stopper was not tight enough, and a new bottle with a different stopper was therefore used. Change of bottle was not done for both bottles as no indications of oxygen were observed before the start.

Figure 4.9 shows the maximum consumption rate per cm^2. The 24 cm^2 had the lowest rate at 0.02 $mmoles/day/cm^2$, close to the rate of 59 cm^2 bottles, while the highest rate was observed for the stirred 14 cm^2 bottles at 0.0. A difference of 0.03 $mmoles/day/cm^2$ from the highest to lowest rate, is not significantly high, meaning the consumption per cm^2 is comparable and does not depend on the total surface area.

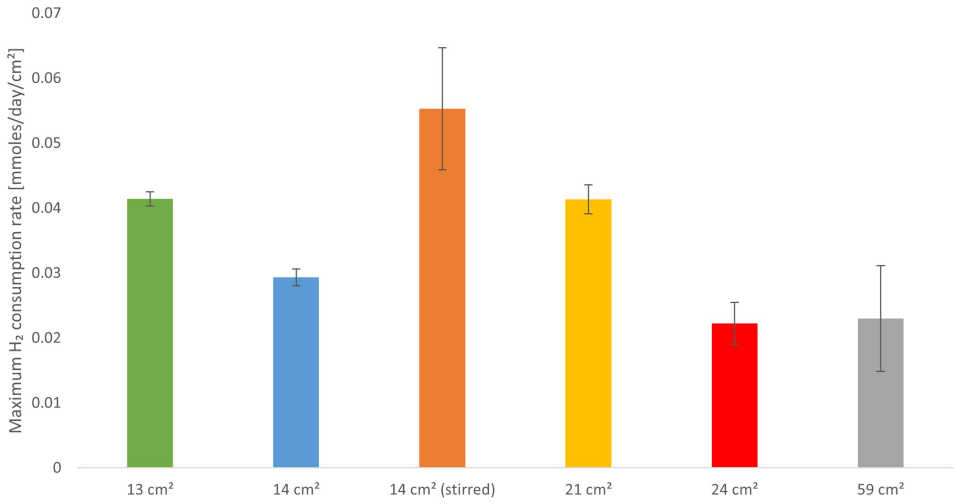

Figure 4.9: Maximum consumption rate per cm^2

When the stirred 14 cm^2 were finished, 6 ml HCl was added to one of the bottles to lower the pH. As explained before, the balance between H_2S and HS^- is pH dependent and acids were added to be able to measure the total amount of H_2S in the bottle. The gas composition of H_2S increased from 5 to 15 % H_2S by lowering the pH, indicating a lot of HS^- in the liquid at the end of the experiment. As for the concentration experiment, H_2S is produced but as the pH increase, H_2S dissolves in liquid to HS^-. This is favorable for UHS as it increases the H_2 purity of the stored gas. Anyhow, the pH development may be different in the reservoir compared to laboratory experiments as other chemicals are present and may affect the pH. Therefore, H_2S is a highly relevant risk related to UHS and more research is needed to fully understand the reservoir-specific pH development.

4.5 pH experiment

MOPS buffers of different concentrations ranging from 1 to 100 mM were used to avoid the rapid pH increase observed in previous experiments. Bottles without MOPS buffer were included in this experiment to compare the pH development and H_2 consumption with the other bottles.

Figure 4.10 shows the relative H_2 consumption for each concentration represented by different colors. During the experiment, the bottles were refilled with gas two times after all H_2 were consumed. For the first part, almost all H_2 was consumed (the rest were expected to be consumed if the sampling continued), and the curves are comparable meaning the H_2 were consumed similarly in all bottles. As the consumption rate is similar, the pH was not affecting the H_2 consumption during this part, even if the pH reached 9 for some of the bottles on day 4. For the second part, the H_2 consumption follows the same rate for the 1, 10, and 100 mM MOPS concentrations, while the 0 mM MOPS concentration

followed the other graphs during the first days before the consumption rate slowed down and differed from the other graphs after some days. At the end of Part 2, some H_2 were not consumed in the 0 mM MOPS concentration bottles when sampling stopped. As the pH was close to the pH of the other bottles it is difficult to conclude the reason for this difference, but as the 0 mM MOPS concentration graph includes large error bars, indicating variations in H_2 consumption between the two duplicates, more optimal growth conditions may explain the variations. For the other MOPS concentrations, almost all H_2 was consumed before sampling stopped. In the third part, the 100 mM MOPS concentration differed from the other graphs. In Figure 4.11 a higher pH for the 100 mM MOPS concentration was observed during the third part, but as the pH was under 9 at the beginning of this part and did not reach 9 until day 56, the pH can not necessarily explain why the graph differed in the beginning. From Figure 4.10 a higher consumption rate for Part 1 compared to Part 2 and 3 can be seen, where Part 3 had the lowest consumption rate.

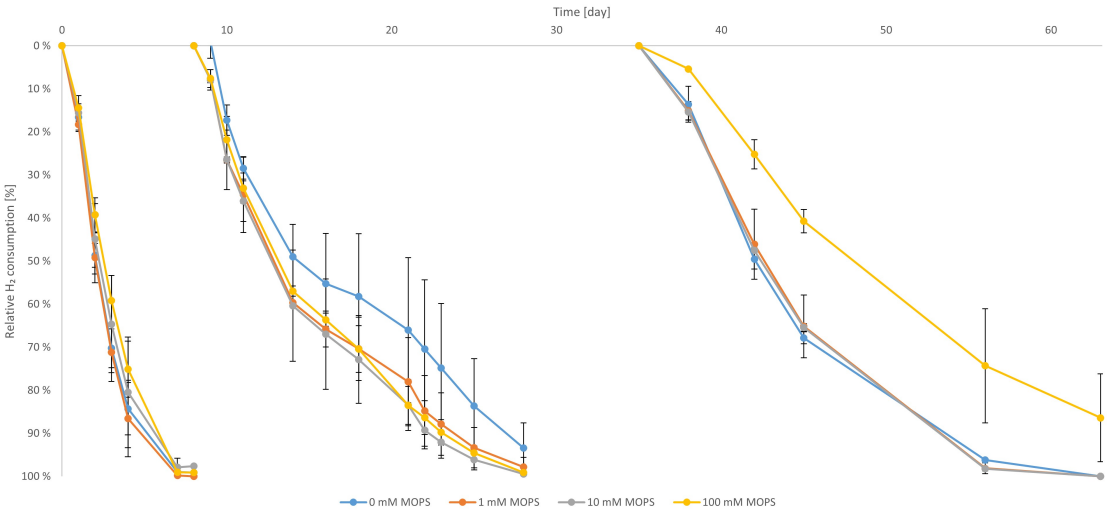

Figure 4.10: Relative H2 consumption where initial MOPS buffer concentrations of 0, 1, 10, and 100 mM are represented. A new part started when the bottles were re-pressurized. The average deviation is represented as the black error bars.

The pH sampled during the experiment can be seen in Figure 4.11. The graphs show a low or no pH effect of the 1 and 10 mM MOPS concentrations, as the pH was similar to the 0 mM MOPS concentration. For the 0, 1, and 10 mM MOPS concentrations the pH increased rapidly the first four days before the pH stabilized. At day 10, MOPS buffer of the same initial concentration was added to the 1 and 10 mM MOPS concentrations, with no or little effect. The next days, a pH increase was observed until day 16 for the 0, 1, and, 10 mM MOPS bottles. On day 18, a small pH decrease was observed before the pH dropped to 7.9 on Day 21. The pH decrease at day 18 can be explained by the new pH meter (see section 3.2.7) used from that day and indicates some errors related

to the other pH meter used before Day 18. At day 21 100 M MOPS buffer was added to both 0, 1, and 10 mM MOPS bottles with the purpose to lower the pH. After adding 100 mM MOPS buffer the pH increased with a lower rate and was kept under 9 until the last days of the experiment. The pH rate differed some for the different concentrations, where the 0 mM MOPS had a higher rate. The pH of the 100 mM MOPS bottles had a lower increasing rate compared to the other bottles and had clearly an effect on the MOPS buffer from the beginning of the experiment. After day 21, when the pH of the other bottles got decreased, the pH of the 100 mM MOPS bottles was higher compared to the others for the rest of the experiment but stayed under 9 until day 45.

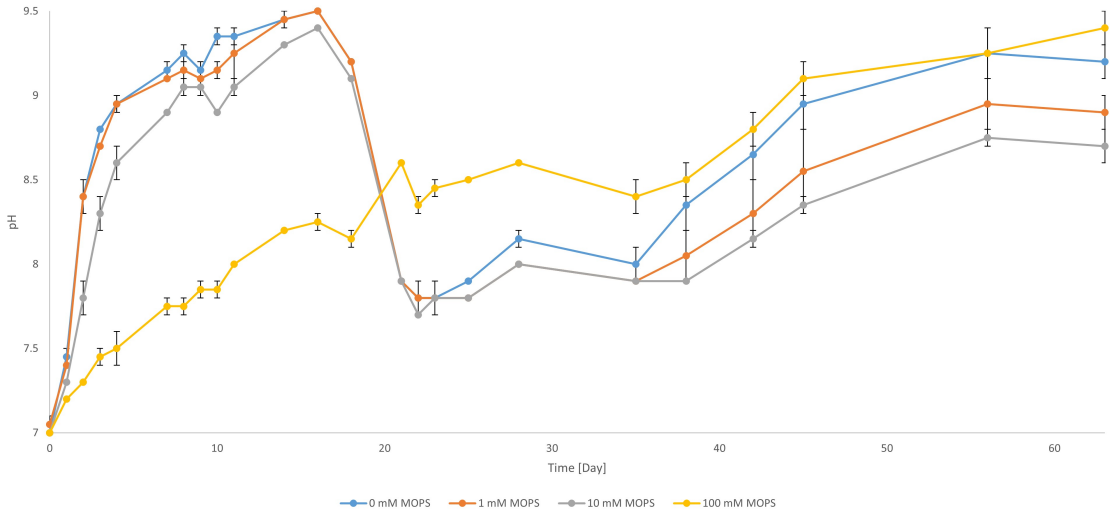

Figure 4.11: Development of pH for the 0, 1, 10, and 100 mM MOPS concentrations. The pH was sampled every sampling day for all three parts of this experiment. The average deviation is represented as the black error bars.

The amount of consumed H_2 in millimoles for each part, as well as the total H_2 consumption for the experiment, is presented in Figure 4.12. As almost all H_2 was consumed for all parts, only small differences in H_2 consumption were observed. These differences in consumption can be explained by differences in the initial amount of H_2 in the bottles or the remaining H_2 in the bottles. The 0 mM MOPS bottles had a higher initial gas volume due to no MOPS buffer (2.5 ml), which may explain why the H_2 consumed in those bottles was higher than the other bottles that had less gas volume. Before this experiment, knowledge about sulfate limitations was established and was added two times (see Figure 4.10) during the experiment to be sure the H_2 consumption did not stop due to sulfate access. As the H_2 consumption continues during the whole experiment, assumptions of sulfate limitations for the other experiments seem to be correct.

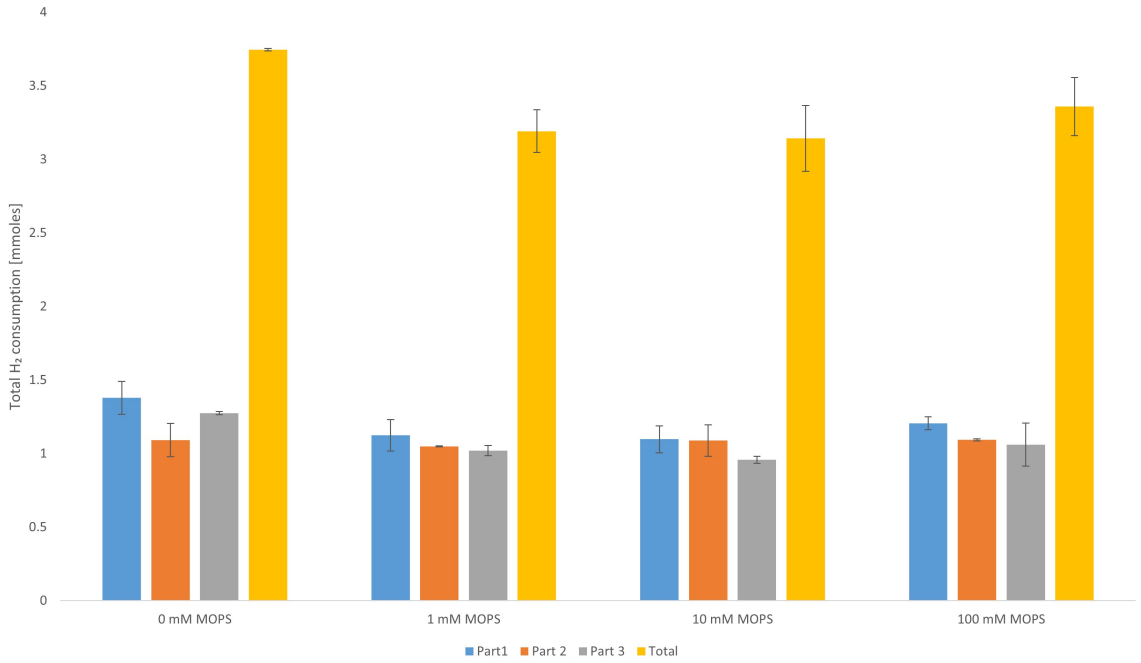

Figure 4.12: Total H_2 consumption in mmoles for separated all parts and the total H_2 consumption for the whole experiment

Table 4.7 summarizes the end pH and the maximum consumption rate in mmoles per day for each part of the experiment. The maximum consumption rate was lower for each part indicating slower H_2 consumption rates for the third part compared to the first part as observed in Figure 4.10. Lower consumption rates may be due to lower microbial activity. For each part, comparable maximum consumption rates were observed for the different MOPS concentrations.

Table 4.7: End pH and maximum consumption rate are given for all parts presented for all bottles.

Bottle	pH (end)	Maximum consumption rate [mmoles/day] (Part 1)	Maximum consumption rate [mmoles/day] (Part 2)	Maximum consumption rate [mmoles/day] (Part 3)
0 mM MOPS	9.2 ± 0.1	0.44 ± 0.01	0.22 ± 0.07	0.11 ± 0.01
1 mM MOPS	8.9 ± 0.1	0.34 ± 0.01	0.20 ± 0.05	0.08 ± 0.02
10 mM MOPS	8.7 ± 0.1	0.33 ± 0.07	0.20 ± 0.02	0.08 ± 0.01
100 mM MOPS	9.4 ± 0.1	0.30 ± 0.05	0.17 ± 0.02	0.07 ± 0.00

Figure 4.13 shows the development of H_2S in the headspace over time. The graphs clearly show the pH impact on the balance between H_2S and HS^-, where higher content of H_2S was observed at lower pH and the opposite. In the beginning, a lower pH was obtained for the 100 mM MOPS concentration and had a higher content of H_2S in the headspace. On day 21, after lowering the pH for the 0, 1, and 10 mM MOPS concentrations, a

rapid H_2S increase was observed. After day 21, a decrease of H_2S was observed for most bottles as the pH increased. Some negative values can be seen for some graphs and are probably related to the uncertainty of the H_2S measurements for the microGC. Again, the pH increase shows a H_2S decrease, favorable for UHS.

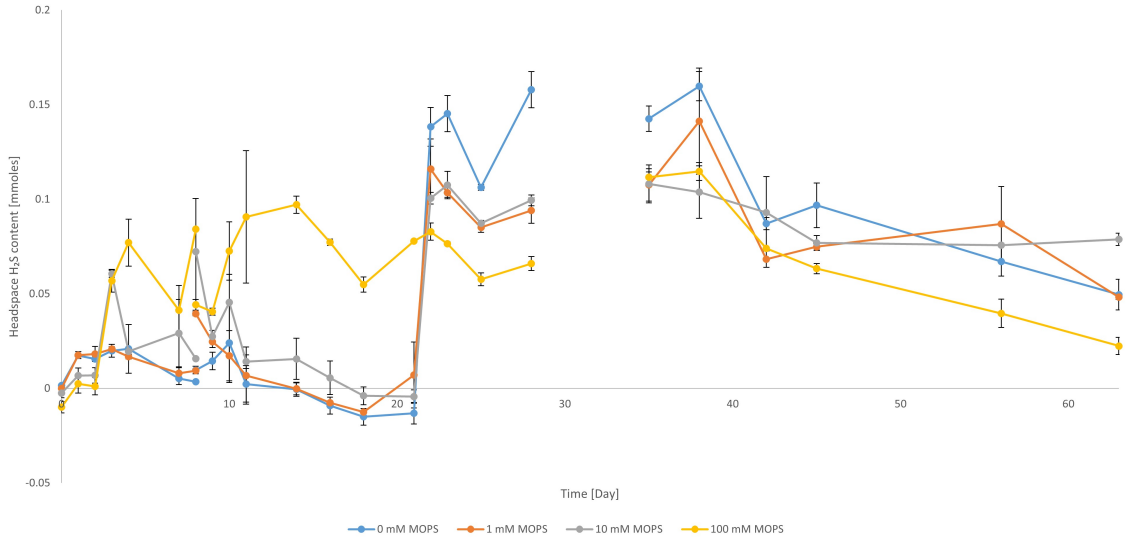

Figure 4.13: H_2S amount in mmoles over time for each MOPS concentration bottle. The variation of H_2S is due to production but also dependence on the pH.

As for the other performed experiments, acetate was not consumed but as acetate was added during Part 2 and 3 with the same amount as initially added, the acetate concentration was approximately tripled at the end of the experiment.

Table 4.8: Acetate concentration in mg/L for some of the bottles at day 0, end part 1 (2 bottles) and end part 3 (all bottles) of the experiment. Samples of two bottles were used to calculate the acetate concentration at day 0 and end part 1.

Day	Bottle	Acetate [mg/L]
Day 0	Bottle 1 and 4	1119 ± 64
End part 1	Bottle 1 and 8	1199 ± 11
End part 3	0 mM MOPS	3183 ± 158
End part 3	1 mM MOPS	2940 ± 44
End part 3	10 mM MOPS	2888 ± 267
End part 3	100 mM MOPS	3317 ± 74

Looking at the result it seemed like *Oleidesulfovibrio alaskensis* was adapting to the environment and found a way to coop with the pH. For UHS this is negative as we want the microbes to be inactive and the H_2 consumption to stop when the pH increase.

4.6 Microbial impact on hydrogen consumption in the porous media

Microfluidics is a field of science and technology that deals with the behavior, control, and manipulation of fluids at the microscale level. It includes the study and design of systems that handle very small volumes of fluids (10^{-9} to 10^{-18} liters) over channels of tens to hundreds micrometers [54]. Microfluidic technology takes advantage of low cost, short analyse time, and minimal experiment footprint and is therefore suitable for research performed at an early stage of a new research topic. Microfluidics utilizes the unique properties of fluids within microchannels, particularly the phenomenon of laminar flow [54]. A micromodel is a microfluidic system used to study mechanisms of fluid behavior within porous media at micro-scales. The micromodel includes a network of connected pores made of transparent material (for example glass or quartz), to be able to observe fluid behavior. A micromodel is usually two-dimensional and has a total size of a few centimeters [55].

A microfluidic experiment using a micromodel was performed to investigate the H_2 consumption of *Oleidesulfovibrio alaskensis* in porous media. The micromodel experiment was performed at the laboratory at the Department of Physics and Technology at the University of Bergen. Dr. Na Liu performed the experiment with the assistance of me and my co-student Kelly Nguyen. Figure 4.14 show the setup for the experiment, where the micromodel is placed to the right, with detailed pictures at the top of the figure. To the left, the hydrogen pump can be seen that was used to inject gas into the micromodel system. A digital camera was used to take images of the micromodel to visualise the hydrogen consumption and behavior of the microbes. This setup used a moveable microscope, able to image the whole micromodel with high resolution. A smaller Field of View (FoV) of the micromodel was focused on when analysing the images. The micromodel images were displayed on the computer and Figure 4.15 shows a full-scale image of the micromodel.

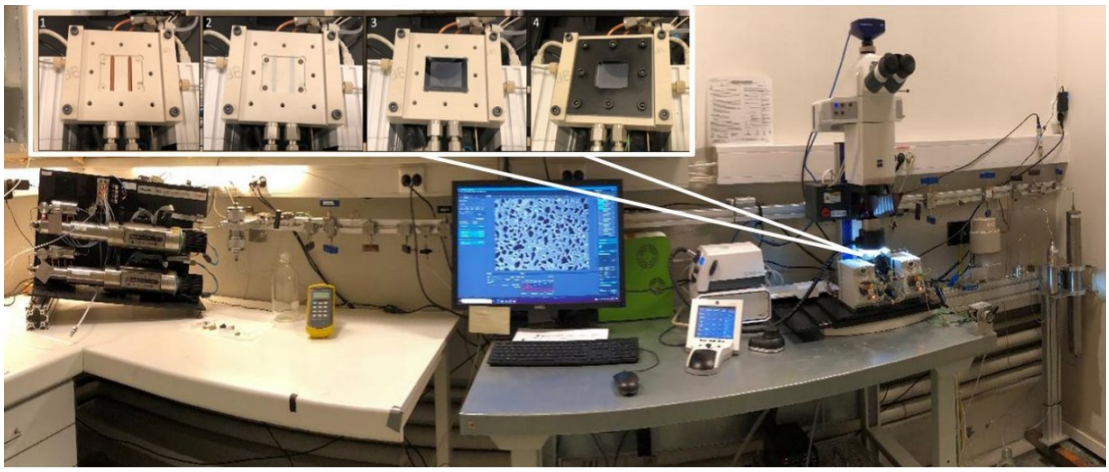

Figure 4.14: The setup for the micromodel experiment. Image provided by Malin Haugen.

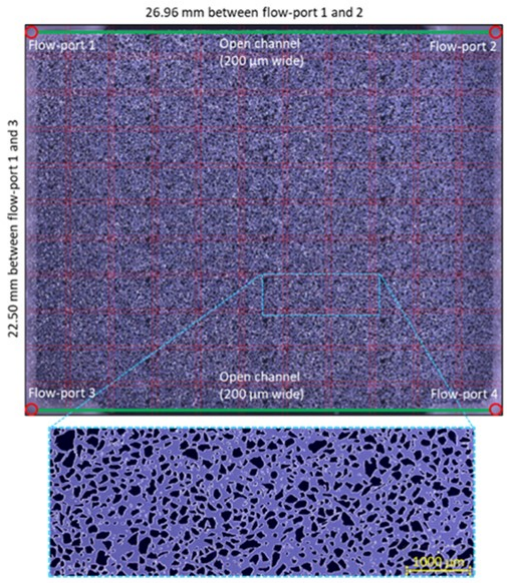

Figure 4.15: Full-scale image of micromodel, including a FoV, provided by Malin Haugen. The H_2 was injected at port 1 and produced at port 4.

A silicon-wafer micromodel including a pore pattern from natural sandstone was used to study the behavior of *Oleidesulfovibrio alaskensis* in a pore scale. A pressure of 5 barg was inserted in the micromodel with a temperature of 37 °C. The conditions represented storage in a shallow aquifer or a gas-water transition zone in a depleted gas field. Details of the experimental setup and procedure can be found in [56]. The procedure performed included some modifications: the pressure was controlled at 5 barg, the bacterial solution included lactate, and the shot-in period lasted for 3 days. The properties of the micromodel are detailed in Table 4.9.

A specific FoV of one single pore was used to analyse the H_2 consumption and microbial behavior. Figure 4.16 shows the development of H_2 consumption and biofilm formation

Table 4.9: Micromodel properties.

Parameter	Value
Width	27.0 mm
Length	21.4 mm
Depth	30 µm
Porosity	0.61
Pore volume	11.1 µL
Permeability	2.97 D
Repetition of pattern	36
Grain size	0.5 - 78 366 μm^2
Pore throat length	0.7 - 194 µm

over 21 hours. The H_2 gas bubble (marked in the 0h image) with a volume of approximately $1.2 \cdot 10^{-6}$ μm^3, decreased over time and was fully consumed after 21 hours. The H_2 gas bubble decreased at a lower rate the first 16 hours before the consumption rate increased and consumed all the remaining H_2 in 5 hours. The consumption rate consists of how microbes are described to grow in the laboratory with a lag phase with low or no microbial growth before the log phase starts and microbial growth increase [36]. The images show the bacteria cells (marked in the 0h image) accumulated at the gas-liquid interface (white light line) or as a water film. *Oleidesulfovibrio alaskensis* formed biofilm over time, marked at the 21h image.

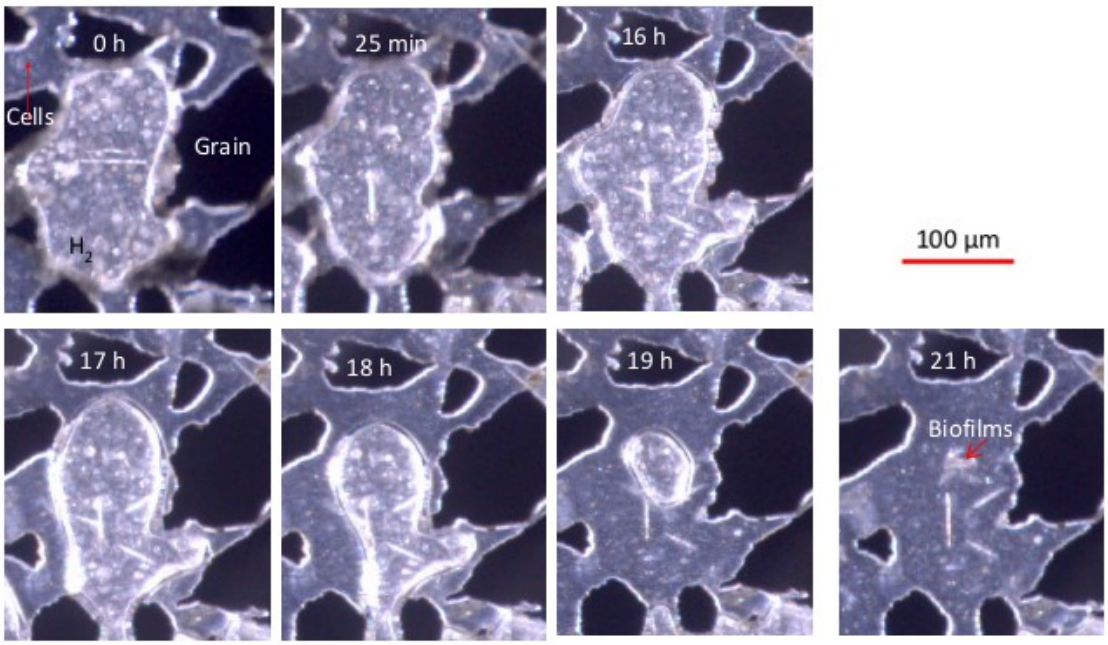

Figure 4.16: H_2 consumption over 21 hours. The gas bubble of H_2, bacteria cells, and grains are marked in the 0h image. Formed biofilms with H_2 can be seen as light and white markings in the 21h image. Images provided by Dr. Na Liu

At this single pore, the H_2 consumption rate was $2.6 \cdot 10^{-13}$ mmoles/day (for calcula-

tions see Appendix C). In a micromodel, the H_2 is surrounded by bacteria solution which causes more consumption of H_2 simultaneously. Nevertheless, the consumption rate in the micromodel was significantly lower than for bottle experiments (0.2 to 0.3 mmoles/day) due to size differences between the studied systems. However, as the bottle experiments always consumed all the available H_2 (when access to sulfate was not limiting), it was assumed the same for the micromodel experiment. At the end of the micromodel experiment, the H_2 consumption stopped even with remaining H_2 in the system (see Figure 4.17). Calculations show that 6.5×10^{-7} moles H_2 can be consumed before all the sulfate was consumed in the micromodel (see Appendix D.2). At Day 0 approximately 6.4×10^{-7} moles of H_2 were in the micromodel, and as not all the H_2 was consumed there had to be sulfate left in the liquid at the end of the experiment. Limiting access to sulfate can not directly explain the zero H_2 consumption, however, lower concentrations of sulfate can decrease the H_2 consumption rate. As micromodels are small-scale systems, there are other factors that may affect the consumption of H_2 compared to the bottle experiment:

- Physical barriers for bacterial movement in the pore structure. Compared to the relatively unobstructed environment of a bottle, physical hindrance can limit bacterial growth and access to H_2 bobbles.

- Differences in microbial cells injected into the system. A volume of 7.77 µL bacterial solution where added to the micromodel, while the bottles had a volume of 25 mL. More microbial cells were therefore available in the bottles compared to the micromodel which may affect the consumption rate.

- Formations of bioproducts and toxins accumulated in the aqueous phase caused by bacterial growth in the micromodel may be unfavorable to continuing microbial growth and could affect the H_2 consumption rate.

- pH may also be a factor limiting microbial growth. The pH was not measured in the micromodel experiment (not feasible), but due to lower liquid volume a higher pH increase may occur causing atop in H_2 consumption.

- Other unknown factors may affect the microbial H_2 consumption and need further investigations.

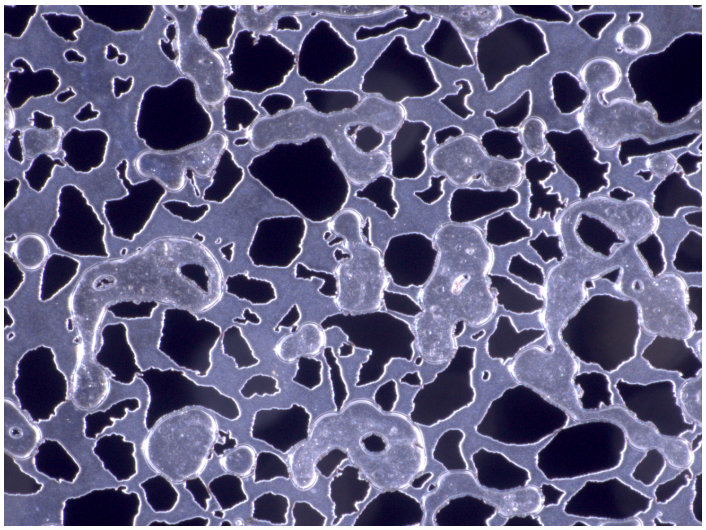

Figure 4.17: FoV of the micromodel showing remaining H_2 in the pores.

As the images show, biofilm was produced over time which may impact the microbial behavior and H_2 consumption. This strain was observed to form a lot of biofilms compared to other bacteria and was observed to cause pore-clogging during bacterial inoculation and H_2 drainage process. In the micromodel, biofilm formation may cause pore-clogging affecting the fluid flow in the system. Coombs *et al.* studied the impact of biofilms in the porous media where biofilms seem to impact both the porosity and permeability of the reservoir [57]. Formation of biofilms in the subsurface depends on factors like access to nutrients, energy sources, and water as well as the presence of microbial cells [57]. Based on this study, biofilm formation is unfavorable for UHS. However, reservoir conditions and access to nutrient and energy sources may be different compared to the conditions in the micromodel and may affect the biofilm formation differently.

As micromodels and laboratory bottles are small scales with limiting volume where microbes grow under optimal culturing conditions, the H_2 consumption rate cannot directly be linked to large-scale systems. In the porous media, other microbes and chemicals will be present, affecting the H_2 consumption and microbial behavior differently. Also, factors like larger volumes, different pressures and temperature may affect the microbial H_2 consumption rate in the subsurface. To assess the extent of reservoir effects, core-scale, and field tests are needed to further estimate the overall positive or negative effects of microbial growth. However, the micromodel and bottle experiments gave an implication of how *Oleidesulfovibrio alaskensis* behave and consume H_2 in the subsurface.

Chapter 5

Conclusion

Laboratory experiments were performed to study the behavior and loss mechanisms related to the sulfate-reducing bacteria *Oleidesulfovibrio alaskensis*. The bottle experiments were performed to investigate how the concentration of H_2 in the stored gas, pressure, surface area, and pH impact the H_2 consumption rate. Micromodel experiments were performed to investigate the behavior and H_2 consumption of the strain in porous media. Key results from performed experiments are summarised below.

Based on the results from bottle experiments, *Oleidesulfovibrio alaskensis* consume H_2 under microbial growth conditions described for this strain. However, the H_2 consumption rate seems to decrease under less optimal conditions where access to nutrients, energy sources, and water were limited for the microbes. For all experiments, a rapid pH increase was observed making the conditions less optimal for microbial growth. However, the microbes seem to continue consuming H_2, even at pH above the maximum growth pH described for this strain, only at a lower rate indicating that these bacterium has found a way to cope with the pH and continue H_2 consumption. Results from the H_2 concentration experiment indicate higher concentrations of H_2 as a better option for UHS as the relative H_2 consumption rate was lower.

Higher pressure and movements in the liquid were assumed to increase the solubility of H_2 and increase the maximum consumption rate. The results indicate no correlation between pressure and maximum H_2 consumption. Presumably, the pressure used was too low to notice this effect, and further investigation is needed. However, higher maximum H_2 consumption rates were observed when stirring the aqueous phase, indicating higher solubility of H_2. Higher maximum H_2 consumption rates were also expected for larger surface areas as more H_2 could be consumed similarly, which was not consistent with the results. Still, the maximum consumption rates per cm^2 were similar for all bottles, indicating the consumption rates per cm^2 too not depend on the surface area.

Results from micromodel experiments gave a lower H_2 consumption rate compared to the bottle experiments due to smaller volumes, and a stop in H_2 consumption was observed. Physical hindrances in the pore structure and production of bioproducts may affect bacterial growth and H_2 consumption. Also, less amount of cells injected in the system or a higher pH increase may cause the stop in H_2 consumption.

Actions are needed to reduce global warming, and UHS offers the possibility of storing large amounts of energy when increasing the shear of renewable energy. However, UHS faces some challenges, and knowledge gaps need to be fulfilled before implementing UHS technology. Subsurface microbes are known for consuming H_2 but knowledge of the microbial impact on H_2 consumption for UHS is not fully understood. Based on the results of this study, *Oleidesulfovibrio alaskensis* seemed to completely consume all available H_2 under optimal conditions for microbial growth, and a way of stopping or decreasing the microbial H_2 consumption has to be investigated. Anyways, the abundance of other microbes and chemicals in the subsurface may impact the microbial H_2 consumption differently and has to be investigated to fully understand the microbial impact on H_2 consumption in the subsurface.

Chapter 6

Future work

Improvements for performed experiments:

- Calculate the total H_2 consumption during the experiments and add sulfate to the bottles when the initial sulfate amount is consumed to improve the results.
- Use a more accurate pH meter to monitor the pH more precisely. Different pH meters were used and indications of error between the pH meters were noticed.
- Follow the pH more frequently for all experiments to get a better understanding of pH evolution.
- Test other H_2 concentration for the H_2 concentration experiment. As the relative consumption for the 40 and 90 % H_2 bottles followed similar trends other H_2 concentrations need to be tested to get a better impression of the suitable gas mixture for UHS.

Further work from performed experiments:

- Cell numbers need to be measured to better understand the microbial growth and H_2 consumption rates.
- Repeat performed experiments to make sure the observed results are consistent.

Other:

- High-pressure experiments have to be performed to investigate the microbial H_2 consumption under conditions more comparable to the storage site pressure.
- Perform similar experiments to other SRBs to get a better impression of how SRB is acting in the subsurface. One single strain can not represent how all SRBs are acting in the subsurface. Research of other strains has to be performed to better understand how SRB behaves and consumes H_2.

- Investigating the microbial activity and H_2 consumption related to other subsurface microbes. A total overview of all subsurface microbes needs to be mapped, to get a better understanding of the microbial activity and H_2 consuming processes in the subsurface.
- Core scale experiments can be performed to investigate the microbial growth under similar conditions to the porous media and more relevant/optimal results will be obtained.
- Fields test will give more relevant results and is needed to predict the microbial influence.

Bibliography

[1] IPCC. , "Summary for Policymakers. In: Climate Change 2022: Mitigation of Climate Change. Contribution of Working Group III to the Sixth Assessment Report of the Intergovernmental Panel on Climate Change," tech. rep., Cambridge University Press, Cambridge, UK and New York, NY, 2022.

[2] H. Ritchie, M. Roser, and P. Rosado, "Energy," *Our World in Data*, 2022.

[3] P. Gabrielli, A. Poluzzi, G. J. Kramer, C. Spiers, M. Mazzotti, and M. Gazzani, "Seasonal energy storage for zero-emissions multi-energy systems via underground hydrogen storage," *Renewable and Sustainable Energy Reviews*, vol. 121, p. 109629, 2020.

[4] D. Gielen, F. Boshell, D. Saygin, M. D. Bazilian, N. Wagner, and R. Gorini, "The role of renewable energy in the global energy transformation," *Energy Strategy Reviews*, vol. 24, pp. 38–50, 2019.

[5] P. Colbertaldo, S. B. Agustin, S. Campanari, and J. Brouwer, "Impact of hydrogen energy storage on California electric power system: Towards 100% renewable electricity," *International Journal of Hydrogen Energy*, vol. 44, no. 19, pp. 9558–9576, 2019.

[6] F. Dawood, M. Anda, and G. M. Shafiullah, "Hydrogen production for energy: An overview," *International Journal of Hydrogen Energy*, vol. 45, no. 7, pp. 3847–3869, 2020.

[7] "Underground Hydrogen Storage: Technology Monitor Report"," tech. rep., Hydrogen TCP-Task 42, 2023.

[8] M. Boudellal, "Power-to-Gas: Renewable Hydrogen Economy for the Energy Transition," in *Power-to-Gas*, De Gruyter, 2018.

[9] L. Louis, "Four Ways to Store Large Quantities of Hydrogen," in *Abu Dhabi International Petroleum Exhibition and Conference*, SPE-208178-MS., 2021.

[10] N. Heinemann, J. Alcalde, J. M. Miocic, S. J. T. Hangx, J. Kallmeyer, C. Ostertag-Henning, A. Hassanpouryouzband, E. M. Thaysen, G. J. Strobel, C. Schmidt-Hattenberger, K. Edlmann, M. Wilkinson, M. Bentham, R. S. Haszeldine, R. Carbonell, and A. Rudloff, "Enabling large-scale hydrogen storage in porous media – the scientific challenges," *Energy & Environmental Science*, vol. 14, no. 2, pp. 853–864, 2021. Publisher: The Royal Society of Chemistry.

[11] R. Tarkowski and B. Uliasz-Misiak, "Towards underground hydrogen storage: A review of barriers," *Renewable and Sustainable Energy Reviews*, vol. 162, p. 112451, 2022.

[12] D. Parra, L. Valverde, F. J. Pino, and M. K. Patel, "A review on the role, cost and value of hydrogen energy systems for deep decarbonisation," *Renewable and Sustainable Energy Reviews*, vol. 101, pp. 279–294, Mar. 2019.

[13] J. D. Fonseca, M. Camargo, J.-M. Commenge, L. Falk, and I. D. Gil, "Trends in design of distributed energy systems using hydrogen as energy vector: A systematic literature review," *International Journal of Hydrogen Energy*, vol. 44, pp. 9486–9504, Apr. 2019.

[14] B. Nastasi and G. Lo Basso, "Power-to-Gas integration in the Transition towards Future Urban Energy Systems," *International Journal of Hydrogen Energy*, vol. 42, pp. 23933–23951, Sept. 2017.

[15] R. Tarkowski, "Underground hydrogen storage: Characteristics and prospects," *Renewable and Sustainable Energy Reviews*, vol. 105, pp. 86–94, 2019.

[16] A. B. Dohrmann and M. Krüger, "Microbial H2 Consumption by a Formation Fluid from a Natural Gas Field at High-Pressure Conditions Relevant for Underground H2 Storage," *Environmental Science & Technology*, vol. 57, pp. 1092–1102, Jan. 2023.

[17] N. Dopffel, S. Jansen, and J. Gerritse, "Microbial side effects of underground hydrogen storage – Knowledge gaps, risks and opportunities for successful implementation," *International Journal of Hydrogen Energy*, vol. 46, no. 12, pp. 8594–8606, 2021.

[18] N. Dopffel and M. B. Nåmdal, "Bridging the gap to a sustainable future: Underground Hydrogen Storage - Norce."

[19] Y. Liu, T. M. Karnauchow, K. F. Jarrell, D. L. Balkwill, G. R. Drake, D. Ringelberg, R. Clarno, and D. R. Boone, "Description of Two New Thermophilic Desulfotomaculum spp., Desulfotomaculum putei sp. nov., from a Deep Terrestrial Subsurface, and Desulfotomaculum luciae sp. nov., from a Hot Spring," *International Journal of Systematic and Evolutionary Microbiology*, vol. 47, no. 3, pp. 615–621, 1997.

[20] B. LibreTexts, "9.3: The Effects of pH on Microbial Growth," in *MICROBIOLOGY*, NICE CXOne, July 2016.

[21] "Bjerrumdiagram - Institutt for biovitenskap." https://www.mn.uio.no/ibv/tjenester/kunnskap/pl

[22] A. I. Osman, N. Mehta, A. M. Elgarahy, M. Hefny, A. Al-Hinai, A. H. Al-Muhtaseb, and D. W. Rooney, "Hydrogen production, storage, utilisation and environmental impacts: A review," *Environmental Chemistry Letters*, vol. 20, pp. 153–188, Feb. 2022.

[23] N. S. Muhammed, B. Haq, D. Al Shehri, A. Al-Ahmed, M. M. Rahman, and E. Zaman, "A review on underground hydrogen storage: Insight into geological sites, influencing factors and future outlook," *Energy Reports*, vol. 8, pp. 461–499, Nov. 2022.

[24] IEA, "The Future of Hydrogen," tech. rep., IEA, Paris, 2019.

[25] M. Hermesmann and T. E. Müller, "Green, Turquoise, Blue, or Grey? Environmentally friendly Hydrogen Production in Transforming Energy Systems," *Progress in Energy and Combustion Science*, vol. 90, p. 100996, May 2022.

[26] IEA. , "Executive summary – Global Hydrogen Review 2021," tech. rep., IEA, Paris, 2021.

[27] M. Noussan, P. P. Raimondi, R. Scita, and M. Hafner, "The Role of Green and Blue Hydrogen in the Energy Transition—A Technological and Geopolitical Perspective," *Sustainability*, vol. 13, p. 298, Jan. 2021.

[28] M. Newborough and G. Cooley, "Developments in the global hydrogen market: The spectrum of hydrogen colours," *Fuel Cells Bulletin*, vol. 2020, pp. 16–22, Nov. 2020.

[29] D. Zivar, S. Kumar, and J. Foroozesh, "Underground hydrogen storage: A comprehensive review," *International Journal of Hydrogen Energy*, vol. 46, pp. 23436–23462, July 2021.

[30] C. R. Matos, J. F. Carneiro, and P. P. Silva, "Overview of Large-Scale Underground Energy Storage Technologies for Integration of Renewable Energies and Criteria for Reservoir Identification," *Journal of Energy Storage*, vol. 21, pp. 241–258, Feb. 2019.

[31] N. Heinemann, J. Scafidi, G. Pickup, E. M. Thaysen, A. Hassanpouryouzband, M. Wilkinson, A. K. Satterley, M. G. Booth, K. Edlmann, and R. S. Haszeldine, "Hydrogen storage in saline aquifers: The role of cushion gas for injection and production," *International Journal of Hydrogen Energy*, vol. 46, pp. 39284–39296, Nov. 2021.

[32] F. Crotogino, S. Donadei, U. Bünger, and H. Landinger, "Large-scale hydrogen underground storage for Securing Future Energy Supplies. 18th World Hydrogen Energy Conference," vol. 78, pp. p. 37–45, 2010.

[33] A. Sainz-Garcia, E. Abarca, V. Rubi, and F. Grandia, "Assessment of feasible strategies for seasonal underground hydrogen storage in a saline aquifer," *International Journal of Hydrogen Energy*, vol. 42, pp. 16657–16666, June 2017.

[34] A. B. Zolotuchin, *Introduction to Petroleum Reservoir Engineering.* Kristiansand: Høyskoleforl, 2000.

[35] S. R. Thiyagarajan, H. Emadi, A. Hussain, P. Patange, and M. Watson, "A comprehensive review of the mechanisms and efficiency of underground hydrogen storage," *Journal of Energy Storage*, vol. 51, p. 104490, July 2022.

[36] D. L. Kirchman, *Processes in Microbial Ecology.* Oxford ; New York: Oxford University Press, 2012.

[37] A. Dutta, S. Dutta Gupta, A. Gupta, J. Sarkar, S. Roy, A. Mukherjee, and P. Sar, "Exploration of deep terrestrial subsurface microbiome in Late Cretaceous Deccan traps and underlying Archean basement, India," *Scientific Reports*, vol. 8, p. 17459, Nov. 2018.

[38] C. Magnabosco, L.-H. Lin, H. Dong, M. Bomberg, W. Ghiorse, H. Stan-Lotter, K. Pedersen, T. L. Kieft, E. van Heerden, and T. C. Onstott, "The biomass and biodiversity of the continental subsurface," *Nature Geoscience*, vol. 11, pp. 707–717, Oct. 2018.

[39] A. Vigneron, E. B. Alsop, B. P. Lomans, N. C. Kyrpides, I. M. Head, and N. Tsesmetzis, "Succession in the petroleum reservoir microbiome through an oil field production lifecycle," *The ISME Journal*, vol. 11, pp. 2141–2154, Sept. 2017.

[40] W. H. Organization, *Laboratory Biosafety Manual, 3rd Edition.* No. WHO/CDS/CSR/LYO/2004.11, 2004.

[41] B. LibreTexts, "9.5: Other Environmental Conditions that Affect Growth," in *MICOBIOLOGY*, July 2016.

[42] S. P. Gregory, M. J. Barnett, L. P. Field, and A. E. Milodowski, "Subsurface Microbial Hydrogen Cycling: Natural Occurrence and Implications for Industry," *Microorganisms*, vol. 7, p. 53, Feb. 2019.

[43] G. Muyzer and A. J. M. Stams, "The ecology and biotechnology of sulphate-reducing bacteria," *Nature Reviews Microbiology*, vol. 6, pp. 441–454, June 2008.

[44] A. Wait and A. Wait, *Novel Aspects of the Reactions of Hydrogenases with Small Molecule Inhibitors*. PhD thesis, Oxford University, UK, 2011.

[45] L. A. Bernardez, L. R. P. de Andrade Lima, E. B. de Jesus, C. L. S. Ramos, and P. F. Almeida, "A kinetic study on bacterial sulfate reduction," *Bioprocess and Biosystems Engineering*, vol. 36, pp. 1861–1869, Dec. 2013.

[46] M. Holmer and H. Hasler-Sheetal, "Sulfide intrusion in seagrasses assessed by stable sulfur isotopes-A synthesis of current results," *Frontiers in Marine Science*, vol. 1, Nov. 2014.

[47] B. LibreTexts, "2.4.2: pH, Buffers, Acids, and Bases," in *MICROBIOLOGY*, May 2017.

[48] M. Feio, V. Zinkevich, I. Beech, E. Llobet-Brossa, P. Eaton, J. Schmitt, and J. Guezennec, "Desulfovibrio alaskensis sp. nov., a sulphate-reducing bacterium from a soured oil reservoir," *International journal of systematic and evolutionary microbiology*, vol. 54, pp. 1747–52, Oct. 2004.

[49] Steris, "Everything About Autoclaves." https://www.steris.com/healthcare/knowledge-center/sterile-processing/everything-about-autoclaves.

[50] N. Hanišáková, M. Vítězová, and S. Rittmann, "The Historical Development of Cultivation Techniques for Methanogens and Other Strict Anaerobes and Their Application in Modern Microbiology," *Microorganisms*, vol. 10, p. 412, Feb. 2022.

[51] V. Koester, "What is HPLC?," June 2016.

[52] "How Fed-Batch Conditions Improve The Quality Of Your Preculture." https://www.scientificbio.com/blog/how-fed-batch-conditions-improve-the-quality-of-your-preculture.

[53] R. R. Ratnakar, B. Dindoruk, and A. Harvey, "Thermodynamic modeling of hydrogen-water system for high-pressure storage and mobility applications," *Journal of Natural Gas Science and Engineering*, vol. 81, p. 103463, Sept. 2020.

[54] G. M. Whitesides, "The origins and the future of microfluidics," *Nature*, vol. 442, pp. 368–373, July 2006.

[55] N. Karadimitriou and S. Hassanizadeh, "A Review of Micromodels and Their Use in Two-Phase Flow Studies," *Vadose Zone Journal*, vol. 11, p. 0, Aug. 2012.

[56] N. Liu, A. R. Kovscek, M. A. Fernø, and N. Dopffel, "Pore-scale study of microbial hydrogen consumption and wettability alteration during underground hydrogen storage," *Frontiers in Energy Research*, vol. 11, 2023.

[57] P. Coombs, D. Wagner, K. Bateman, H. Harrison, A. Milodowski, D. Noy, and J. West, "The role of biofilms in subsurface transport processes," *Quarterly Journal of Engineering Geology and Hydrogeology*, vol. 43, pp. 131–139, May 2010.

Appendices

Appendix A

HPLC procedure

This chapter provides the HPLC procedure and details the instruments used for this analyse. The procedure was written and provided by Dr. Abduljelil Kedir. HPLC is a method to analyse the content of a liquid and was used to measure the concentration of acetate in this study. The procedure was performed by Dr. Abduljelil Kedir at NORCE main office in Bergen who also performed the calculations. Figure A.1 and A.2 were used for the calculations.

suplied the data Procedure:
Liquid samples were analyzed by using liquid chromatography of Agilent 1260II HPLC which is equipped with a quaternary pump, temperature control column compartment integrated with autosampler, 1260 Refractive Index Detector (RID), and 1260 Diode Array Detectors HS (DAD HS). A guard column (i.e., Hi-Plex H 50X7.7mm) and an analytical column (i.e., Hi-Plex H 300 x 7.7 mm, 8μm) were used for the separation of the analytes. Milli-Q water was used to prepare the mobile phase, solutions, and samples after filtering it through a 0.22μm Millipak filter. A mobile phase of 14 mM H2SO4 solution was prepared from HPLC grade stock solution and run in isocratic elution mode. Samples are diluted by using mobile phase solution (i.e., 14 mM H2SO4) and filtered through using a 0.45 μm RC syringe filter. A 20 µL of the sample was injected and the total run time was between 40 to 75 min depending on analyte interest. The autosampler compartment was controlled at 22°C while the column temperature was maintained at 60°C.

The organic acids were monitored using DAD and RID while sugars and alcohols were monitored using RID. The DAD recorded the absorbance at a wavelength of 210 nm beside the spectrum between 190-400 nm. The RID optical unit temperature was set to 55°C with positive polarity mode and the reference cell was purged with the mobile phase before starting the analysis. The column was conditioned at 0.2 mL/min and 60°C with Milli-Q water overnight and regenerated with 14mM H2SO4 for 2 hours after every

batch of analysis. This protocol is to extend the durability of the analytical column besides using the guard column. The Agilent OpenLAB CDS Software was used for data acquisition and data processing. All analytes were identified and quantified based on retention time and the respective reference standard calibration curves.

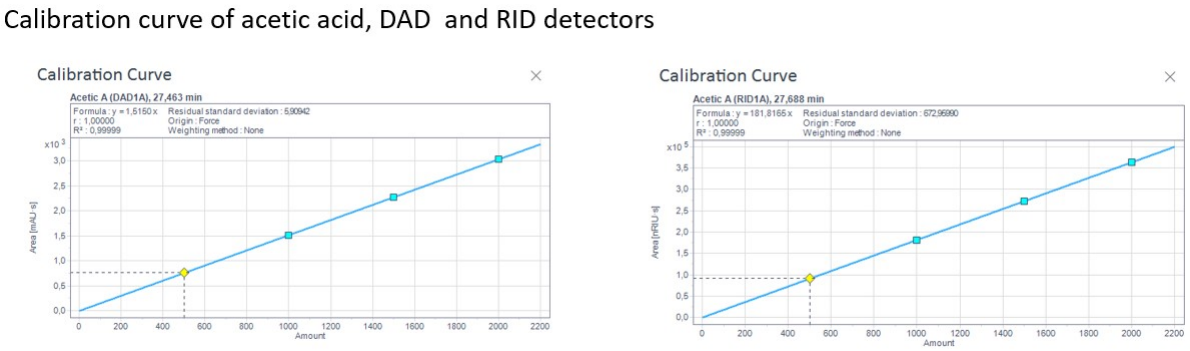

Figure A.1: Calibration curve of acetic acid, DAD and RID detectors

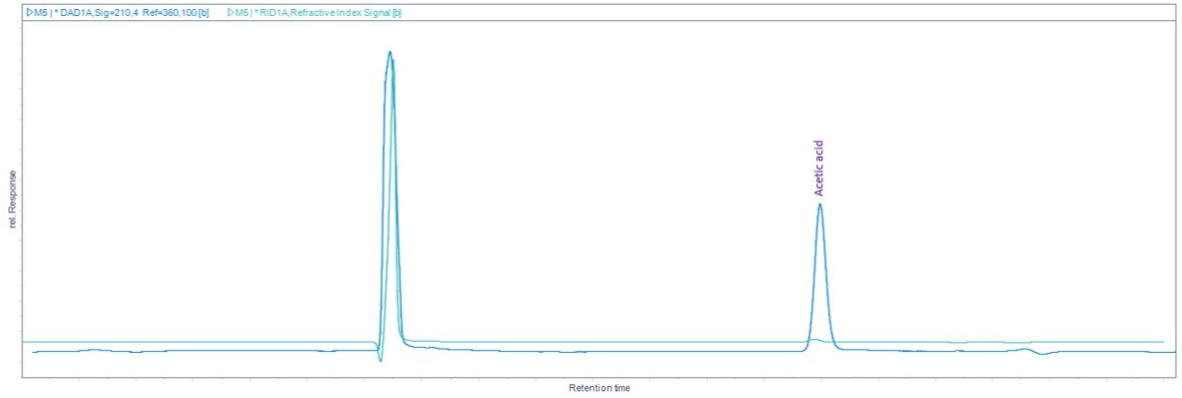

Figure A.2: Chromatogram

Appendix B

Pressure and gas composition data

This chapter gives an example of how raw data of sampled pressure (Figure B.1) and gas composition (Figure B.2) looks. The examples are from the hydrogen concentration experiment and were used to calculate the amount of H_2 and H_2S in the bottles using the ideal gas law (Equation 3.2).

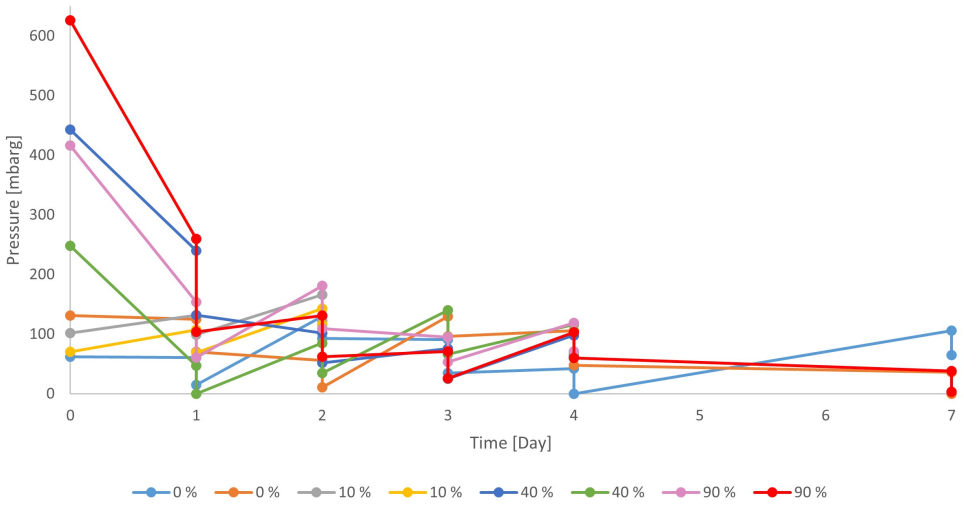

Figure B.1: Pressure data from the H_2 concentration experiment fro unssterile bottles. The pressure was sampled twice a day.

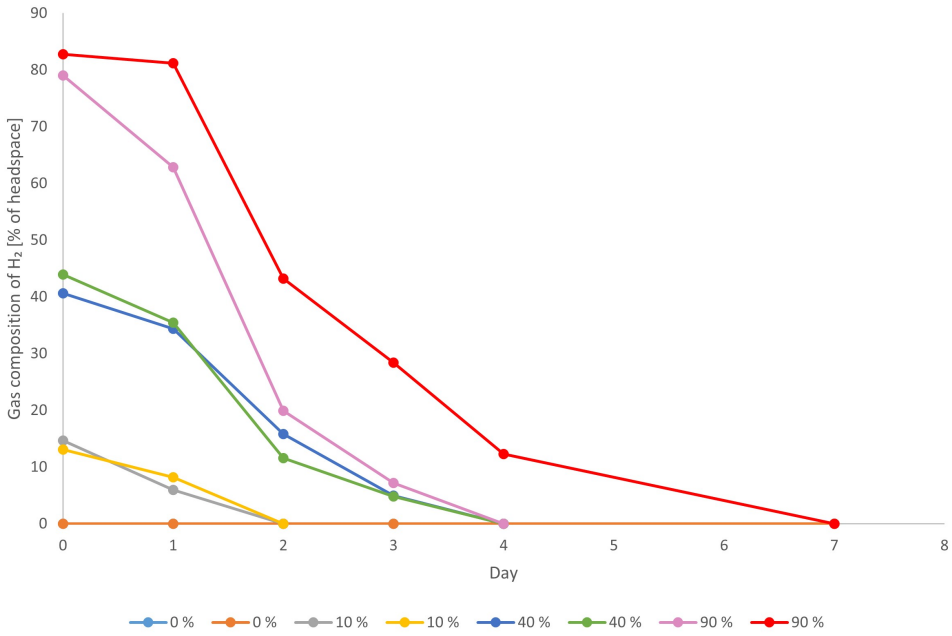

Figure B.2: H_2 gas composition data from the H_2 concentration experiment for unsterile bottles.

Appendix C

Calculations for micromodel experiment

This chapter details the calculations performed to estimate the H_2 consumption rate of the H_2 in Figure 4.16. The volume of H_2 at day 0 was $1.2 \cdot 10^{-6} \mu m^3$ calculated and provided by Dr. Na Liu. Table C.1 gives the density of H_2 at 37 °C and 5 bar and the molar mass of H_2.

Table C.1: Overview of H_2 density and molar mass

H_2 density at 37 °C and 5 bar	0.00039 g/mL
Molar mass H_2	2.016 g/mol

As it took 21 hours before the H_2 gas in that pore was consumed, the consumption rate was calculated to be 56284.28 $\mu m^3/h$ by dividing the initial volume of H_2 on time used for consumption. By multiplying the consumption rate by the density and dividing it by the molecular weight, the consumption rate was calculated to be 2.6 mmoles/day (see Table C.2).

Table C.2: H_2 consumption rate for the micromodel experiment.

Consumption rate	Unit
$5.62 \cdot 10^{-4}$	$\mu m^3/h$
$1.35 \cdot 10^{-6}$	ml/day
$5.27 \cdot 10^{-10}$	g/day
$2.61 \cdot 10^{-10}$	moles/day
$2.61 \cdot 10^{-13}$	mmoles/day

Appendix D

Sulfate calculations

This chapter will show how to calculate how much H_2 that can be consumed before all the available sulfate in the bottles and micromodel is consumed.

D.1 Bottle experiment

There was 3 g Sodium sulfate (Na_2SO_4) per L medium, and Na_2SO_4 has a molecular weight of 142.04 g/mol. By using Equation D.1, there was calculated a concentration of SO_4 at 21.1 mM in the medium.

$$Molarity = \frac{\rho}{Mm} \tag{D.1}$$

ρ is the density of the solution while Mm is the molecular weight.

For SRB, 4 H_2 molecules are consumed per 1 SO_4 molecule (see Tabel 2.2), meaning that 21.1 mM So_4 consumes 84.4 mM H_2. The number of moles of H_2 consumed was calculated using Equation D.2, where n is the number of moles, v is the volume of the solution (25 mL) and c is the concentration of H_2.

$$n = v * c \tag{D.2}$$

With a volume of 25 mL and a concentration of 84.4 mM, 21 mmoles H_2 can be consumed before all SO_4 is consumed.

D.2 Micromodel experiment

For the micromodel experiment, the liquid volume was 7.7 µL with the same concentration of sulfate. To consume all the available sulfate $6.5 \cdot 10^{-7}$ moles of H_2 must be

consumed.